Journal Pre-proof

Model-based meta-analysis to optimise *S. aureus*-targeted therapies for atopic dermatitis

Takuya Miyano, Alan D. Irvine, Reiko J. Tanaka

PII: S2667-0267(22)00017-0

DOI: https://doi.org/10.1016/j.xjidi.2022.100110

Reference: XJIDI 100110

To appear in: *JID Innovations*

Received Date: 18 October 2021

Revised Date: 18 January 2022

Accepted Date: 25 January 2022

Please cite this article as: Miyano T, Irvine AD, Tanaka RJ, Model-based meta-analysis to optimise *S. aureus*-targeted therapies for atopic dermatitis, *JID Innovations* (2022), doi: https://doi.org/10.1016/j.xjidi.2022.100110.

Model-based meta-analysis to optimise *S. aureus*-targeted therapies for atopic dermatitis

Short title: Model analysis to target *S. aureus* in eczema

Takuya Miyano[1], Alan D Irvine[2,3] and Reiko J Tanaka[1*]

1 Department of Bioengineering, Imperial College London, UK

2 Pediatric Dermatology, Children's Health Ireland at Crumlin, Dublin

3 Clinical Medicine, Trinity College Dublin, Dublin, Ireland

*Corresponding author: Reiko J. Tanaka

Department of Bioengineering, Imperial College London

South Kensington Campus, London, SW7 2AZ, UK

+44 20 7594 6374

r.tanaka@imperial.ac.uk

Twitter account: @TanakaGroup

ORCID ID

TM: 0000-0002-1181-6924; ADI: 0000-0002-9048-2044; RJT: 0000-0002-0769-9382

Abbreviations

AD: atopic dermatitis

agr: accessory gene regulatory

AIPs: autoinducing peptides

AMPs: antimicrobial peptides

CoNS: Coagulase Negative Staphylococcus

EASI: Eczema Area and Severity Index

MoA: Mechanism of action

PSMs: phenol-soluble modulins

QSP: quantitative systems pharmacology

S. aureus: *Staphylococcus aureus*

*Sh*A9: *Staphylococcus hominis* A9

ABSTRACT

Several clinical trials of *Staphylococcus aureus* (*S. aureus*)-targeted therapies for atopic dermatitis (AD) have demonstrated conflicting results regarding whether they improve AD severity scores. This study performs a model-based meta-analysis to investigate possible causes of these conflicting results and suggests how to improve the efficacies of *S. aureus*-targeted therapies.

We developed a mathematical model that describes systems-level AD pathogenesis involving dynamic interactions between *S. aureus* and Coagulase Negative *Staphylococcus* (CoNS). Our model simulation reproduced the clinically observed detrimental effects of application of *S. hominis* A9 (*Sh*A9) and flucloxacillin on AD severity and showed that these effects disappeared if the bactericidal activity against CoNS was removed. A hypothetical (modelled) eradication of *S. aureus* by 3.0 $\log_{10}$ CFU/cm^2, without killing CoNS, achieved comparable EASI-75 to dupilumab. This efficacy was potentiated if dupilumab was administered in conjunction with *S. aureus* eradication (EASI-75 at week 16; *S. aureus* eradication: 66.7%, dupilumab 61.6% and combination: 87.8%). The improved efficacy was also seen for virtual dupilumab poor responders.

Our model simulation suggests that killing CoNS worsens AD severity and that *S. aureus*-specific eradication without killing CoNS could be effective for AD patients, including dupilumab poor responders. This study will contribute to design promising *S. aureus*-targeted therapy.

KEYWORDS: atopic dermatitis, clinical efficacy, model-based meta-analysis, quantitative systems pharmacology, *Staphylococcus aureus*

INTRODUCTION

Atopic dermatitis (AD), also called eczema, is the most common inflammatory skin disease (Deckers et al., 2012). The symptoms of AD involve relapsing pruritus and skin pain, which impairs patients' quality of life and work productivity (Simpson et al., 2016a). The pathogenesis of AD is characterised by skin barrier damage, Th2-dominant inflammation and skin dysbiosis (Czarnowicki et al., 2019; Langan et al., 2020; Weidinger et al., 2018). The most well understood skin dysbiosis in AD patients is colonisation by *Staphylococcus aureus* (*S. aureus*) and a decreased relative abundance of commensal bacteria in the skin (Ederveen et al., 2019). *S. aureus* skin colonisation is found in 75%-90% of AD patients without clinical signs of superinfection, whereas it is found in only 0%-25% of healthy subjects (Breuer et al., 2002; Gong et al., 2006; Park et al., 2013; Higaki et al., 1999; Nath, et al., 2020).

S. aureus colonisation density correlates with AD severity (Callewaert et al., 2020; Cau et al., 2021), and *S. aureus* has been considered as a promising target for AD treatment as it induces both skin barrier damage and inflammation by producing various virulence factors, such as phenol-soluble modulins (PSMs), staphylococcal enterotoxins and the toxic shock syndrome toxin-1 (Syed et al., 2015; Geoghegan et al., 2018).

Some clinical trials of *S. aureus*-targeted therapies for AD have indeed demonstrated a reduction in *S. aureus* densities (Tham et al., 2020). They have, however, shown conflicting results as to whether they improve AD severity scores. For example, in several clinical trials, oral and topical anti-staphylococcal antibiotics were applied to eradicate *S. aureus* at least temporarily on AD skin lesions. These interventions, however, often failed to improve AD severity: A Cochrane review concluded that antibiotics may make no difference or only slight improvement in AD severity (George et al., 2019). Oral flucloxacillin, one of the antibiotics, worsened AD severity compared to placebo despite a significant reduction of *S. aureus* levels on skin lesion (Ewing et al., 1998). Currently, the use of antibiotics is recommended for AD only in case of overt infection (Alexander et al., 2020; Le Poidevin et al., 2019).

As another *S. aureus*-targeted therapy: transplant of *S. hominis* A9 (*Sh*A9), a commensal strain of coagulase-negative staphylococci (CoNS) isolated from healthy human skin, has been tested (Nakatsuji et al., 2021a). A clinical study showed that *Sh*A9 transplant decreased the *S. aureus* levels on skin lesions and improved AD severity scores in the patients (*N*=21) whose skin was colonised with *S. aureus* that is sensitive to the bacteriocins secreted by *Sh*A9. However, the *Sh*A9 transplant worsened AD severity scores in the patients (*N*=11) whose skin was colonised with *S. aureus* resistant to the bacteriocins secreted by *Sh*A9 (Nakatsuji et al., 2021a). *Sh*A9 produces bacteriocins with bactericidal activity against *S.*

aureus (Nakatsuji et al., 2017) and secretes autoinducing peptides (AIPs) that inhibit the accessory gene regulatory (agr) system, which regulates the expression of the virulence factors in *S. aureus* (Williams et al., 2019).

Some therapeutics that do not target *S. aureus* directly can also reduce *S. aureus* levels. Dupilumab, an approved biologic for AD, is a monoclonal antibody that inhibits IL-4 and IL-13 signalling. These Th2 cytokines can facilitate *S. aureus* colonisation as they damage the skin barrier by inhibiting epidermal differentiation (Seltmann et al., 2015; Howell et al., 2009);skin barrier damage induces an increase in skin pH (Elias. 2017) that promotes *S. aureus* growth (Lambers et al., 2006). In addition, inhibition of IL-4 and IL-13 by dupilumab can reduce *S. aureus* levels since IL-4 and IL-13 inhibit the synthesis of antimicrobial peptides (AMPs) against *S. aureus* (Howell et al., 2006). Dupilumab has been shown to reduce *S. aureus* levels and improve AD severity scores in a clinical trial (Callewaert et al., 2020).

Taken together, flucloxacillin, *Sh*A9 and dupilumab decreased *S. aureus* levels but showed contrasting efficacies with respect to improved AD severity scores. Understanding the underlying mechanism for these contrasting efficacies will help optimise consistently effective *S. aureus*-targeted therapies for AD.

To investigate the causes of the conflicting efficacies of *S. aureus*-targeted therapies, this study applies a quantitative systems pharmacology (QSP) approach. QSP is a framework to describe systems-level pathogenesis and treatment effects by integrating data and knowledge into a mathematical model (Schoeberl et al., 2019). A QSP approach facilitates a model-based meta-analysis that integrates data from different clinical trials, as well as knowledge on pathogenesis and mechanism of action (MoA) of treatments, to inform rational drug development (Gibbs et al., 2018). A QSP model-based meta-analysis is especially suitable for this study which aims to investigate underlying mechanisms for the conflicting efficacies of *S. aureus*-targeted therapies observed in different clinical studies.

We have recently applied a QSP model-based meta-analysis of multiple biologics for AD and identified IL-13 and IL-22 as potential drug targets for dupilumab poor responders (Miyano et al., 2021). However, the previous QSP model of biologics is not suitable for this study's aim as it did not describe the mechanism of *S. aureus*-targeted therapies. This study presents a new QSP model of *S. aureus*-targeted therapies that describes the interactions between *S. aureus* and CoNS in AD pathogenesis by referring to clinical efficacy data of the three treatments described above (flucloxacillin, *Sh*A9 and dupilumab. The selection process is detailed in Supplementary Information (SI) Section 1) to test the following two hypotheses.

Our first hypothesis is that the bactericidal effects of *S. aureus*-targeted therapies on CoNS impair their efficacies on AD severity. Decrease in CoNS levels causes reduction in their AIP secretion, thereby upregulating agr expression. Upregulated agr expression promotes production of virulence factors in *S. aureus* that can worsen AD severity. While such a hypothesis has already been implied in several studies (Nakatsuji et al., 2021a; Clowry et al., 2019; Katsuyama et al., 2005), there has been no quantitative evaluation on the possible dynamic influences of killing CoNS on clinical efficacies to the best of our knowledge.

The second hypothesis is that *S. aureus*-targeted therapies are effective for dupilumab poor responders as they have a different MoA from dupilumab. The responder rates for dupilumab were 44%-69% (Simpson et al., 2016b; Blauvelt et al., 2017) for Eczema Area and Severity Index (EASI)-75 (75% reduction in the EASI score (Hanifin et al., 2001; Schram et al., 2012)), leaving a significant proportion of dupilumab poor responders. Therapeutic options for dupilumab poor responders are limited to increasing topical corticosteroids and adding additional systemic immunosuppressive agents. However, dupilumab poor responders are often resistant to these treatments and require monitoring for adverse effects (Hendricks et al., 2019), leaving unmet medical needs for dupilumab poor responders. This paper proposes promising *S. aureus*-targeted therapies for AD patients, especially for dupilumab poor responders, by conducting model simulations on virtual patients.

RESULTS

QSP model reproduced clinical efficacies of three treatments that decreased *S. aureus* levels

We normalised *S. aureus* levels, EASI scores and EASI-75 using the reported results in clinical trials to compare efficacies of flucloxacillin, *Sh*A9 and dupilumab (FIGURE 1 and SI Section 2). Efficacies of *Sh*A9 were presented for two groups of patients stratified by the sensitivity of their *S. aureus* to *Sh*A9 bacteriocins, as in the original clinical study (Nakatsuji et al., 2021a). Hereafter, *Sh*A9 applied to patients colonised with *S. aureus* that is sensitive to *Sh*A9 bacteriocins is referred as *Sh*A9-sensitive, and those with *S. aureus* that is resistant to *Sh*A9 bacteriocins is referred as *Sh*A9-resistant.

The normalised efficacies demonstrated that all the treatments decreased *S. aureus* levels and that *Sh*A9-sensitive and dupilumab improved the EASI scores and EASI-75, whereas *Sh*A9-resistant and flucloxacillin worsened the EASI scores and EASI-75. The results confirmed that the three treatments demonstrated conflicting efficacies on AD severity scores while they all reduced *S. aureus* levels.

We revised our previously published QSP model of biologics (Miyano et al., 2021) to include the MoA for the three treatments and interactions between *S. aureus* and CoNS (FIGURE 2 and SI Section 3). The new QSP model of *S. aureus*-targeted therapies reproduced the baseline levels of the biological factors and the clinical efficacies of the treatments on *S. aureus* levels, EASI scores and EASI-75 (FIGURE 3a, b and SI Section 4). The root mean square errors of the mean and %CV of *S. aureus* levels, the EASI scores and EASI-75 between the simulated and reference data were 0.3 $\log_{10}$ CFU/cm^2, 43%, 1.5 (out of 72 = the maximal EASI score) and 2.9%, respectively.

Detrimental effects of flucloxacillin and *Sh*A9 on EASI scores disappeared when their bactericidal activity against CoNS was hypothetically removed

Using the new QSP model, we tested the first hypothesis that the bactericidal effects on CoNS impair the efficacies of *S. aureus*-targeted therapies on AD severity.

Our model simulation demonstrated that flucloxacillin and *Sh*A9-resistant decreased CoNS while increasing the agr expression (FIGURE 3c) and that flucloxacillin and *Sh*A9 could achieve better EASI scores and EASI-75 than placebo if they had no bactericidal effects on CoNS (FIGURE 4). In addition, a sensitivity analysis of the model parameters for %improved EASI demonstrated that lower rates of CoNS killing by flucloxacillin (d_{fh}) and *Sh*A9 (d_{A9h}) result in higher %improved EASI (SI Section 5). These results suggested that a decrease in CoNS increases agr expression, thereby worsening EASI scores.

While CoNS levels were reduced to similar levels in both the *Sh*A9-sensitive and *Sh*A9-resistant groups, agr expression was reduced only in the *Sh*A9-sensitive group (FIGURE 3c). The agr expression decreased due to the stronger decrease of *S. aureus* levels by *Sh*A9-sensitive, compared to *Sh*A9-resistant, even though the decrease in CoNS resulted in a slight increase in the agr expression. These results suggest that the efficacies of *S. aureus*-targeted therapies are determined in some part by the balance of their bactericidal strengths against *S. aureus* vs. CoNS.

Hypothetical *S. aureus*-targeted therapies achieved better EASI-75 than dupilumab

The QSP model described antimicrobial effects of *S. aureus*-targeted therapies by three parameters: the rate of *S. aureus* killing, that of CoNS killing and the strength of agr expression inhibition (FIGURE 2). The antimicrobial effects result in a decrease of *S. aureus* levels, that of CoNS level and an inhibition of agr expression level, respectively (FIGURE 5a).

To explore which antimicrobial effects are responsible for improvement in AD severity, we conducted model simulations for hypothetical *S. aureus*-targeted therapies with different values of the three parameters.

Our simulation results demonstrated that lower *S. aureus* levels, higher CoNS levels and stronger inhibition of agr expression resulted in higher EASI-75 after 16 weeks (FIGURE 5b left). The *S. aureus*-specific eradication (the maximal reduction of *S. aureus* level without killing CoNS, yellow arrows in FIGURE 5b) led to comparable EASI-75 to dupilumab (66.7% vs. dupilumab: 61.6%). The EASI-75 of the *S. aureus*-specific eradication was improved by adding 90% inhibition of the agr expression (70.6%, blue arrows in FIGURE 5b).

Simulations for a combinatorial application of dupilumab and hypothetical *S. aureus*-targeted therapies elucidated that it can achieve better EASI-75 than an application of either one (FIGURE 5b right). The *S. aureus*-specific eradication improved EASI-75 (87.8%) when it was combined with dupilumab, which was further improved (91.9%) by adding 90% inhibition of agr expression.

S. aureus-targeted therapies achieved significant responses in virtual dupilumab poor responders

We also simulated EASI-75 of *S. aureus*-targeted therapies in dupilumab poor responders (FIGURE 5c). Similar to the results shown above for all virtual patients (FIGURE 5b), lower *S. aureus* levels, higher CoNS levels and higher inhibition of agr expression showed a better EASI-75 in virtual dupilumab poor responders. The hypothetical *S. aureus*-specific eradication achieved a significant EASI-75 in virtual dupilumab poor responders (*S. aureus*-specific eradication: 43.2% and that with 90% inhibition of agr expression: 61.1%), which were potentiated by simultaneous application of dupilumab (*S. aureus*-specific eradication: 61.5% and that with 90% inhibition of agr expression: 79.6%).

DISCUSSION

QSP model-based meta-analysis reveals mechanism of conflicting efficacies of *S. aureus*-targeted therapies

We developed a QSP model that describes the interactions between *S. aureus* and CoNS in AD pathogenesis (FIGURE 2) by integrating data and knowledge from published experiments using human samples (SI Section 3). The model reproduced published data of clinical efficacy for flucloxacillin, *Sh*A9 and dupilumab (FIGURE 1) regarding the EASI scores, EASI-75 and *S. aureus* levels (FIGURE 3).

The QSP model simulation revealed that *S. aureus*-targeted therapies can worsen the EASI scores if they kill CoNS. The simulation showed that the application of *Sh*A9 and flucloxacillin had detrimental effects on AD severity, and those effects disappeared if their bactericidal activity against CoNS was hypothetically removed (FIGURE 4). A schematic of the QSP model (FIGURE 2) can explain how a decrease in CoNS impairs the EASI scores. The decreased CoNS levels diminish secreted AIPs, thereby upregulating the agr expression. The upregulated agr expression promotes the production of virulence factors that damage the skin barrier (e.g., by PSMα and enterotoxins) and induce inflammation (e.g., by wall teichoic acid to activate dendritic cells), which can worsen AD severity. These results and interpretation indicate an importance of bactericidal specificity on *S. aureus* in *S. aureus*-targeted therapies.

Model simulation quantifies relationships between profiles of antibacterial effects and responder rates

The QSP model simulation enables quantitative discussion on clinical efficacies of hypothetical therapies, which cannot be achieved using only qualitative models (FIGURE 2). Our simulation elucidated quantitative relationships between antibacterial effects of *S. aureus*-targeted therapies (decreases in the *S. aureus* and CoNS levels and in the agr expression level) and their EASI-75 responder rates (FIGURE 5b left). In addition, our simulation suggested that the efficacy of *S. aureus*-targeted therapies can be potentiated by concomitant use of dupilumab (FIGURE 5b right).

Theoretically, *S. aureus*-targeted therapies will achieve the best efficacy if they eradicated *S. aureus* completely. However, some *S. aureus* may remain on population average after *S. aureus*-targeted therapies, presumably due to resistance to antibiotics and bacteriocins (Harkins et al., 2019). Hence, it is crucial to inhibit agr expression by keeping the AIPs produced by CoNS, in addition to killing *S. aureus,* to minimise the agr-dependent virulence effects of *S. aureus*.

Hypothetical *S. aureus*-specific eradication (the maximal reduction of *S. aureus* level without killing CoNS), especially in combination with dupilumab, showed higher responder rates than dupilumab alone (Simulated EASI-75 at week 16: placebo 26.6%, dupilumab 61.6%, *S. aureus*-specific eradication 66.7% and combination 87.8%. FIGURE 5b right). Recently, JAK inhibitors have demonstrated promising efficacies in AD patients; abrocitinib showed a comparable response to dupilumab (EASI-75 at week 16; abrocitinib 71.0% vs. dupilumab 65.5%, not significant) (Bieber et al., 2021)[0], and upadacitinib showed the highest responder rate among Ph3 trials of JAK inhibitors (EASI-75 at week 16. upadacitinib 77.1% vs. placebo 26.4%) (Reich et al., 2021)[0]. Our simulation implies that *S. aureus*-specific eradication combined with dupilumab may achieve higher responder rates than JAK inhibitors. These quantitative comparison of clinical efficacies between hypothetical and existing therapies is one of the benefits of model simulation.

S. aureus-specific eradication is potentially effective for dupilumab poor responders

Another benefit of model simulation is that it can compute expected clinical efficacies of hypothetical therapies in specific subpopulations. This study also suggested the effectiveness of *S. aureus*-specific eradication for dupilumab poor responders. Simulation for virtual dupilumab poor responders showed that *S. aureus*-specific eradication achieved 43.2% EASI-75 (FIGURE 5c left), which is much higher than EASI-75 achieved (up to 33.8%) when we simulated inhibition of all the cytokines considered in the previous QSP model of biologics (Miyano et al., 2021). These results imply that *S. aureus,* rather than cytokines, is potentially a promising therapeutic target for dupilumab poor responders.

The model simulation also demonstrated that the efficacy of *S. aureus*-targeted therapies is potentiated by its concomitant use with dupilumab in dupilumab poor responders (FIGURE 5c right). The results suggest that IL-4/IL-13 signalling contributes to the pathogenesis even for dupilumab poor responders and thus needs to be inhibited. Targeting both *S. aureus* and IL-4/IL-13 could be a promising therapeutic approach for AD patients.

Limitation of the QSP model simulation

This study aimed to interpret published clinical data on *S. aureus*-targeted therapies obtained under different study conditions using a model-based meta-analysis. We assumed their efficacies are comparable across clinical trials after normalisation, although the study conditions (e.g., topical and systemic therapies) may influence the reported efficacies. For example, one of the clinical trials (Nakatsuji et al., 2021a) evaluated efficacies of *Sh*A9 for a short period (10 days), posing uncertainty on its long-term efficacy. Accuracy of the simulated

efficacies of the hypothetical *S. aureus*-targeted therapies needs to be verified by future clinical trials (Cucurull-Sanchez et al., 2019).

We made our model as simple as possible to concisely interpret clinical efficacies of *S. aureus*-targeted therapies with reference to AD pathogenesis. There are several factors that our model omitted as they were not relevant in this study. For example, our model approximates pharmacokinetics as a switch-like behaviour (treatment effects are ON at the start of dosing and are OFF at the end of dosing). Modelling of AD pathogenesis considered the cutaneous compartment of skin lesions (e.g., without considering cytokines in blood), excluded potential roles of other microbes than *S. aureus* and CoNS, does not explicitly describe some biological factors such as AMPs and immune cells, and simplified some pathways (e.g., IL-4 and IL-13 increase *S. aureus* and CoNS via decreasing AMPs, where AMPs were not described as a model variable). Our model could be further expanded when those omitted factors become relevant for specific investigation.

Our model assumed that CoNS has no detrimental effects on the skin barrier and inflammation. However, recent studies have suggested that *S. epidermidis*, one of CoNS, also has detrimental effects on the skin barrier (Cau et al., 2021). The detrimental effects of *S. epidermidis* may explain the worsened EASI scores in *Sh*A9 as it increased the proportion of *S. epidermidis* among microbiome in the AD skin lesion (Nakatsuji et al., 2021a). Explicit modelling of different CoNS strains may deliver further insights into the roles of CoNS in AD pathogenesis, although our model assumed the detrimental effects of *S. epidermidis* are negligible compared to those of *S. aureus* because *S. aureus* has a higher correlation with AD severity scores than *S. epidermidis* (Ederveen et al., 2019; Byrd et al., 2017).

Prospect for *S. aureus*-targeted therapies

The results of this study support the widely accepted idea that *S. aureus* is a promising drug target for AD and suggests the potential importance of considering antibacterial activities against both *S. aureus* and CoNS when developing *S. aureus*-targeted therapies. How much *S. aureus* killing is required to achieve a set efficacy for any given therapy would depend on how strongly the therapy kills CoNS and inhibits agr expression.

This study presents an example of how QSP model can contribute to model-informed drug development (EFPIA MID3 Workgroup et al., 2016) for precision medicine. For example, our simulation results will contribute to the design of *S. aureus*-targeted therapies because the simulated relationship between EASI-75 responder rates and antibacterial effects (i.e., decreases in the *S. aureus* and CoNS levels and inhibition of agr expression) can be used

as a guide to set a target profile of the antibacterial effects to achieve a desirable efficacy (e.g., better EASI-75 than dupilumab). Our simulation results also encourage combinatorial use of *S. aureus*-targeted therapies and cytokine-targeted therapies such as biologics and JAK inhibitors for AD.

METHODS

Our QSP model explicitly describes causal relationships between treatments, biological factors and an AD severity score using a graphical scheme and ordinary differential equations. The model was developed by 1) selecting treatments and biological factors to be modelled, 2) formulating treatment effects and causal relationships between the biological factors and 3) optimising model parameters that define virtual patients. The developed model was used to simulate the clinical efficacies of hypothetical *S. aureus*-targeted therapies in virtual patients.

Selecting treatments and biological factors

We considered flucloxacillin, *Sh*A9 and dupilumab because they demonstrated a decrease of *S. aureus* levels in a placebo-controlled double-blinded clinical study where AD severity scores were reported (Table 1 and SI Section 1).

We selected six biological factors as model variables: colony density levels of *S. aureus* and CoNS and levels of agr expression, IL-4/IL-13 in the skin and skin barrier integrity and the EASI score (TABLE S2). *S. aureus* and CoNS are the core factors in this study. “CoNS” does not include the *Sh*A9 strain applied in the *Sh*A9 treatment. “Agr expression*”* corresponds to the main mechanism for *S. aureus* to expression virulence factors in *S. aureus* (Williams et al., 2019) that induce skin barrier damage and skin inflammation. The IL-4/IL-13 represents Th2-cytokines that are targeted by dupilumab. “Skin barrier integrity” is a critical factor in AD pathogenesis as in our previous models (Miyano et al., 2021; Domínguez-Hüttinger et al., 2017). The EASI score represents an endpoint for AD severity. Some biological factors such as AMPs were not described as model variables but were considered implicitly as a rationale for the causal relationships (e.g., IL-4 and IL-13 increase *S. aureus* and CoNS via decreasing AMPs) to make the model simpler yet interpretable.

Formulating treatment effects and causal relationships between biological factors

We developed a mathematical model consisting of six equations corresponding to the six biological factors with 26 parameters to simulate the efficacies of the three treatments (SI Section 3). The effects of flucloxacillin were modelled by increasing the killing rates of both

S. aureus and CoNS as its antibacterial spectrum covers all Staphylococcus species. The effects of *Sh*A9 were modelled by increasing the killing rates of *S. aureus* and CoNS and the inhibitory strength against the agr expression because *Sh*A9 produces bacteriocins against both *S. aureus* and CoNS (Nakatsuji et al., 2017) and AIPs that inhibit the agr expression (Nakatsuji et al., 2021a). The effects of dupilumab were modelled by decreasing effective concentrations of IL-4/IL-13 in the skin by 99%. The value of 99% was obtained from a calculation using the published data on IC_{50} and the mean concentration of drugs in the skin (Vazquez et al., 2018) that was estimated from their concentration in the serum measured in clinical trials (SI Section 3.2.3). The causal relationships between biological factors were described according to published experimental evidence based on human data (SI Section 3.1). The model was implemented in Python 3.7.6 (Python Software Foundation).

Modelling virtual patients and optimising model parameters

We assumed that the model parameter values (e.g., the recovery rate of skin barrier via skin turnover, k_1) vary between AD patients and that a set of 26 parameter values defines pathophysiological backgrounds of each virtual patient (TABLE S3). Each value of the i-th parameter, k_i, is taken from a log-normal distribution (Limpert et al., 2001) whose probability function, $f(k_i)$, is defined by

$$f(k_i) = \frac{1}{\sqrt{2\pi}\sigma_i k_i} \exp\left(-\frac{(\ln k_i - \mu_i)^2}{2\sigma_i^2}\right), \quad (1)$$

where μ_i and σ_i are the distribution parameters that represent the mean and the standard deviation of $\ln k_i$, respectively.

We optimised the 52 distribution parameters (μ_i and σ_i, i=1, …, 26) that define distributions of the 26 model parameters so that the model minimises root mean square errors of both mean values and standard deviations between simulated data and the reference data derived from published clinical studies (SI Section 4). The reference data consist of baseline levels of *S. aureus*, CoNS, IL-4/IL-13 and the EASI scores (TABLE S2) and time courses of *S. aureus* levels, EASI scores and EASI-75 assessed in clinical trials of the selected treatments (FIGURE 1). The *S. aureus* levels, EASI scores and EASI-75 were normalised to compare the clinical efficacies of different clinical trials (SI Section 2). agr expression and skin barrier integrity were regarded as latent state variables that have no reference data to be compared with simulated values. Simulated baseline levels were obtained by computing steady-state levels of biological factors (at 1000 weeks without treatment). All the simulations were conducted on 1000 virtual patients generated by randomly sampling each parameter value

from the distribution in Eq. (1).

Simulating efficacies of hypothetical *S. aureus*-targeted therapies

We simulated EASI-75 of hypothetical therapies with different strengths for killing of *S. aureus* and of CoNS and for inhibiting agr expression to explore optimal *S. aureus*-targeted therapies. Specifically, we examined the efficacies of hypothetical therapies that achieve a maximal reduction of *S. aureus* level from placebo (a reduction of 3.0 $\log_{10}$ CFU/cm^2; the reported maximal reduction is 3.1 $\log_{10}$ CFU/cm^2 by cefuroxime axetil (Boguniewicz et al., 2001) and neomycin (Leyden and Kligman, 1977) among published clinical trials for *S. aureus*-targeted therapies (Ewing et al., 1998; Nakatsuji et al., 2021a; Boguniewicz et al., 2001; Leyden and Kligman, 1977; Hung et al. 2007; Korting et al., 1994; Breneman et al., 2000)), the maximal level of CoNS (no bactericidal effects on CoNS, keeping the baseline level of CoNS), an example level of inhibition of the agr expression (we used 90% as we have no reliable evidence to estimate maximal inhibition rates of agr expression) and their combinations.

We also simulated EASI-75 of hypothetical therapies in virtual dupilumab poor responders, which were defined as the virtual patients who did not achieve the EASI-75 criterion at 16 weeks.

Data Availability Statement

The code of the QSP model is available at https://github.com/Tanaka-Group/AD_QSP_model.

Conflict of Interest Statement

Takuya Miyano reports personal fees from DAIICHI SANKYO CO., LTD., during the conduct of the study, outside the submitted work; Alan D Irvine reports personal fees from Sanofi Regeneron, personal fees from AbbVie, personal fees from Eli Lilly, personal fees from Pfizer, personal fees from UCB Pharma, personal fees from Novartis, personal fees from Dermavant, personal fees from Benevolent AI, personal fees from Menlo Therapeutics, personal fees from Chugai, personal fees from LEO Pharma, personal fees from Arena, during the conduct of the study, all outside the submitted work; Reiko J Tanaka reports grants from British Skin Foundation, during the conduct of the study.

Acknowledgments

We thank Dr. Elisa Domínguez-Hüttinger for her insightful comments on our manuscript.

Funding Information

This work was funded by the British Skin Foundation (005/R/18).

Author Contributions Statement

Conceptualization: TM, RJT; Data curation: TM; Formal Analysis: TM; Funding acquisition: RJT; Investigation: TM; Methodology: TM; Project administration: RJT; Resources: RJT; Software: TM; Supervision: RJT; Validation: TM; Visualization: TM; Writing – original draft: TM, RJT; Writing – review & editing: TM, ADI, RJT

REFERENCES

Alexander H, Paller AS, Traidl-Hoffmann C, et al. The role of bacterial skin infections in atopic dermatitis: expert statement and review from the International Eczema Council Skin Infection Group. Br J Dermatol. 2020;182(6):1331-42.

Amin K. The role of mast cells in allergic inflammation. Respir Med. 2012;106(1):9-14

Azimi E, Reddy VB, Lerner EA. Brief communication: MRGPRX2, atopic dermatitis and red man syndrome. Itch (Phila). 2017;2(1):e5.

Becker K, Haverkämper G, von Eiff C, Roth R, Peters G. Survey of staphylococcal enterotoxin genes, exfoliative toxin genes, and toxic shock syndrome toxin 1 gene in non-Staphylococcus aureus species. Eur J Clin Microbiol Infect Dis. 2001;20(6):407-9.

Bieber T, Simpson EL, Silverberg JI, et al. Abrocitinib versus Placebo or Dupilumab for Atopic Dermatitis. N Engl J Med. 2021;384(12):1101-12.

Blauvelt A, de Bruin-Weller M, Gooderham M, et al. Long-term management of moderate-to-severe atopic dermatitis with dupilumab and concomitant topical corticosteroids (LIBERTY AD CHRONOS): a 1-year, randomised, double-blinded, placebo-controlled, phase 3 trial. Lancet. 2017;389:2287-303

Bohl T. Lichenification Superimposed on an Underlying Preceding Pruritic Disease. Vulvar Disease. 2019:153-5.

Boguniewicz M, Sampson H, Leung SB, Harbeck R, Leung DY. Effects of cefuroxime axetil on Staphylococcus aureus colonization and superantigen production in atopic dermatitis. J Allergy Clin Immunol. 2001;108(4):651-2.

Breneman DL, Hanifin JM, Berge CA, Keswick BH, Neumann PB. The effect of antibacterial soap with 1.5% triclocarban on Staphylococcus aureus in patients with atopic dermatitis. Cutis. 2000;66(4):296-300.

Breuer K, HAussler S, Kapp A, Werfel T. Staphylococcus aureus: colonizing features and influence of an antibacterial treatment in adults with atopic dermatitis. Br J Dermatol. 2002;147(1):55-61.

Byrd AL, Deming C, Cassidy SKB, et al. Staphylococcus aureus and Staphylococcus epidermidis strain diversity underlying pediatric atopic dermatitis. Sci Transl Med. 2017;9(397):eaal4651.

Callewaert C, Nakatsuji T, Knight R, et al. IL-4Rα Blockade by Dupilumab Decreases Staphylococcus aureus Colonization and Increases Microbial Diversity in Atopic Dermatitis. J Invest Dermatol. 2020;140(1):191-202.e7.

Cau L, Williams MR, Butcher AM, et al. Staphylococcus epidermidis protease EcpA can be a deleterious component of the skin microbiome in atopic dermatitis. J Allergy Clin Immunol. 2021;147(3):955-66.e16.

Clowry J, Irvine AD, McLoughlin RM. Next-generation anti-Staphylococcus aureus vaccines: A potential new therapeutic option for atopic dermatitis?. J Allergy Clin Immunol. 2019;143(1):78-81.

Cucurull-Sanchez L, Chappell MJ, Chelliah V, et al. Best Practices to Maximize the Use and Reuse of Quantitative and Systems Pharmacology Models: Recommendations From the United Kingdom Quantitative and Systems Pharmacology Network. CPT Pharmacometrics Syst Pharmacol. 2019;8(5):259-72.

Czarnowicki T, He H, Krueger JG, Guttman-Yassky E. Atopic dermatitis endotypes and implications for targeted therapeutics. J Allergy Clin Immunol. 2019;143:1-11

de Wit J, Totté JEE, van Mierlo MMF, et al. Endolysin treatment against Staphylococcus aureus in adults with atopic dermatitis: A randomized controlled trial. J Allergy Clin Immunol. 2019;144(3):860-3.

Deckers IA, McLean S, Linssen S, Mommers M, van Schayck CP, Sheikh A. Investigating international time trends in the incidence and prevalence of atopic eczema 1990-2010: a systematic review of epidemiological studies. PLoS One. 2012;7:e39803

D'Ippolito D, Pisano M. Dupilumab (Dupixent): An Interleukin-4 Receptor Antagonist for Atopic Dermatitis. P T. 2018;43(9):532-5

Domínguez-Hüttinger E, Christodoulides P, Miyauchi K, et al. Mathematical modeling of atopic dermatitis reveals "double-switch" mechanisms underlying 4 common disease phenotypes. J Allergy

Clin Immunol. 2017;139:1861-72.e7

dos Santos Nascimento J, Fagundes PC, de Paiva Brito MA, dos Santos KR, do Carmo de Freire Bastos M. Production of bacteriocins by coagulase-negative staphylococci involved in bovine mastitis. Vet Microbiol. 2005;106(1-2):61-71.

Ederveen THA, Smits JPH, Hajo K, et al. A generic workflow for Single Locus Sequence Typing (SLST) design and subspecies characterization of microbiota. Sci Rep. 2019;9(1):19834.

EFPIA MID3 Workgroup, Marshall SF, Burghaus R, et al. Good Practices in Model-Informed Drug Discovery and Development: Practice, Application, and Documentation. CPT Pharmacometrics Syst Pharmacol. 2016;5:93-122

Elias PM. The how, why and clinical importance of stratum corneum acidification. Exp Dermatol. 2017;26(11):999-1003.

Ewing CI, Ashcroft C, Gibbs AC, Jones GA, Connor PJ, David TJ. Flucloxacillin in the treatment of atopic dermatitis. Br J Dermatol. 1998;138(6):1022-9.

Foelster Holst R, Reitamo S, Yankova R, et al. The novel protease inhibitor SRD441 ointment is not effective in the treatment of adult subjects with atopic dermatitis: results of a randomized, vehicle-controlled study. Allergy. 2010;65(12):1594-9.

Geoghegan JA, Irvine AD, Foster TJ. Staphylococcus aureus and Atopic Dermatitis: A Complex and Evolving Relationship. Trends Microbiol. 2018;26(6):484-97.

George SM, Karanovic S, Harrison DA, et al. Interventions to reduce Staphylococcus aureus in the management of eczema. Cochrane Database Syst Rev. 2019;2019(10):CD003871.

Gibbs JP, Menon R, Kasichayanula S. Bedside to Bench: Integrating Quantitative Clinical Pharmacology and Reverse Translation to Optimize Drug Development. Clin Pharmacol Ther. 2018;103(2):196-8

Gong JQ, Lin L, Lin T, et al. Skin colonization by Staphylococcus aureus in patients with eczema and atopic dermatitis and relevant combined topical therapy: a double-blind multicentre randomized controlled trial. Br J Dermatol. 2006;155(4):680-7.

Grossmann M, Jamieson MJ, Kirch W. Histamine response and local cooling in the human skin: involvement of H1- and H2-receptors. Br J Clin Pharmacol. 1999;48(2):216-22

Gueniche A, Knaudt B, Schuck E, et al. Effects of nonpathogenic gram-negative bacterium Vitreoscilla filiformis lysate on atopic dermatitis: a prospective, randomized, double-blind, placebo-controlled clinical study. Br J Dermatol. 2008;159(6):1357-63.

Guttman-Yassky E, Blauvelt A, Eichenfield LF, et al. Efficacy and Safety of Lebrikizumab, a High-Affinity Interleukin 13 Inhibitor, in Adults With Moderate to Severe Atopic Dermatitis: A Phase 2b Randomized Clinical Trial. JAMA Dermatol. 2020;156(4):411-20

Guttman-Yassky E, Bissonnette R, Ungar B, et al. Dupilumab progressively improves systemic and cutaneous abnormalities in patients with atopic dermatitis. J Allergy Clin Immunol. 2019a;143(1):155-72.

Guttman-Yassky E, Pavel AB, Zhou L, et al. GBR 830, an anti-OX40, improves skin gene signatures and clinical scores in patients with atopic dermatitis. J Allergy Clin Immunol. 2019b;144(2):482-93.e7

Hanifin JM, Thurston M, Omoto M, Cherill R, Tofte SJ, Graeber M. The eczema area and severity index (EASI): assessment of reliability in atopic dermatitis. EASI Evaluator Group. Exp Dermatol. 2001;10:11-8

Harkins CP, Holden MTG, Irvine AD. Antimicrobial resistance in atopic dermatitis: Need for an urgent rethink. Ann Allergy Asthma Immunol. 2019;122(3):236-40.

Hendricks AJ, Lio PA, Shi VY. Management Recommendations for Dupilumab Partial and Non-durable Responders in Atopic Dermatitis. Am J Clin Dermatol. 2019;20:565-9

Higaki S, Morohashi M, Yamagishi T, Hasegawa Y. Comparative study of staphylococci from the skin of atopic dermatitis patients and from healthy subjects. Int J Dermatol. 1999;38(4):265-9.

Howell MD, Boguniewicz M, Pastore S, et al. Mechanism of HBD-3 deficiency in atopic dermatitis. Clin Immunol. 2006;121(3):332-8

Howell MD, Kim BE, Gao P, et al. Cytokine modulation of atopic dermatitis filaggrin skin expression. J Allergy Clin Immunol. 2009;124(3 Suppl 2):R7-12

Hung SH, Lin YT, Chu CY, et al. Staphylococcus colonization in atopic dermatitis treated with fluticasone or tacrolimus with or without antibiotics. Ann Allergy Asthma Immunol. 2007;98(1):51-6.

Jack RW, Tagg JR, Ray B. Bacteriocins of gram-positive bacteria. Microbiol Rev. 1995;59(2):171-200.

Katsuyama M, Kobayashi Y, Ichikawa H, Mizuno A, Miyachi Y, Matsunaga K, Kawashima M. A novel method to control the balance of skin microflora Part 2. A study to assess the effect of a cream containing farnesol and xylitol on atopic dry skin. J Dermatol Sci. 2005 Jun;38(3):207-13.

Kabashima K, Matsumura T, Komazaki H, Kawashima M; Nemolizumab-JP01 Study Group. Trial of Nemolizumab and Topical Agents for Atopic Dermatitis with Pruritus. N Engl J Med. 2020;383(2):141-50

Koppes SA, Brans R, Ljubojevic Hadzavdic S, Frings-Dresen MH, Rustemeyer T, Kezic S. Stratum Corneum Tape Stripping: Monitoring of Inflammatory Mediators in Atopic Dermatitis Patients Using Topical Therapy. Int Arch Allergy Immunol. 2016;170(3):187-93

Korting HC, Zienicke H, Braun-Falco O, et al. Modern topical glucocorticoids and anti-infectives for superinfected atopic eczema: do prednicarbate and didecyldimethylammoniumchloride form a rational combination?. Infection. 1994;22(6):390-4.

Kwaszewska A, Sobiś-Glinkowska M, Szewczyk EM. Cohabitation--relationships of corynebacteria and staphylococci on human skin. Folia Microbiol (Praha). 2014;59(6):495-502.

Lambers H, Piessens S, Bloem A, Pronk H, Finkel P. Natural skin surface pH is on average below 5, which is beneficial for its resident flora. Int J Cosmet Sci. 2006;28(5):359-70.

Lane P. Handling drop-out in longitudinal clinical trials: a comparison of the LOCF and MMRM approaches. Pharm Stat. 2008;7(2):93-106.

Langan SM, Irvine AD, Weidinger S. Atopic dermatitis. Lancet. 2020;396:345-360.

Weidinger S, Beck LA, Bieber T, Kabashima K, Irvine AD. Atopic dermatitis. Nat Rev Dis Primers.

2018;4:1

Le Floc'h A, Allinne J, Nagashima K, et al. Dual blockade of IL-4 and IL-13 with dupilumab, an IL-4Rα antibody, is required to broadly inhibit type 2 inflammation. Allergy. 2020;75(5):1188-204

LePoidevin LM, Lee DE, Shi VY. A comparison of international management guidelines for atopic dermatitis. Pediatr Dermatol. 2019;36(1):36-65.

Leung DY, Harbeck R, Bina P, et al. Presence of IgE antibodies to staphylococcal exotoxins on the skin of patients with atopic dermatitis. Evidence for a new group of allergens. J Clin Invest. 1993;92(3):1374-80.

Leung TH, Zhang LF, Wang J, Ning S, Knox SJ, Kim SK. Topical hypochlorite ameliorates NF-κB-mediated skin diseases in mice. J Clin Invest. 2013;123(12):5361-70.

Leung DY. Atopic dermatitis: new insights and opportunities for therapeutic intervention. J Allergy Clin Immunol. 2000;105(5):860-76

Leyden JJ, Kligman AM. The case for steroid--antibiotic combinations. Br J Dermatol. 1977;96(2):179-87.

Limpert E, Stahel WA, Abbt M. Log-normal distributions across the sciences: keys and clues: on the charms of statistics, and how mechanical models resembling gambling machines offer a link to a handy way to characterize log-normal distributions, which can provide deeper insight into variability and probability-normal or log-normal: that is the question. BioScience. 2001;51:341-52

Marino S, Hogue IB, Ray CJ, Kirschner DE. A methodology for performing global uncertainty and sensitivity analysis in systems biology. J Theor Biol. 2008;254:178-96

Menzies BE, Kenoyer A. Staphylococcus aureus infection of epidermal keratinocytes promotes expression of innate antimicrobial peptides. Infect Immun. 2005;73(8):5241-4

Miyano T, Irvine AD, Tanaka RJ. A mathematical model to identify optimal combinations of drug targets for dupilumab poor responders in atopic dermatitis. [e-pub ahead of print]. Allergy. 2021. doi:10.1111/all.14870 (accessed 10 January 2022).

Myles IA, Earland NJ, Anderson ED, et al. First-in-human topical microbiome transplantation with Roseomonas mucosa for atopic dermatitis. JCI Insight. 2018;3(9):e120608.

Nakatsuji T, Chen TH, Narala S, et al. Antimicrobials from human skin commensal bacteria protect against Staphylococcus aureus and are deficient in atopic dermatitis. Sci Transl Med. 2017;9(378):eaah4680.

Nakatsuji T, Hata TR, Tong Y, et al. Development of a human skin commensal microbe for bacteriotherapy of atopic dermatitis and use in a phase 1 randomized clinical trial. Nat Med. 2021a;27(4):700-9.

Nakatsuji T, Gallo RL, Shafiq F, et al. Use of Autologous Bacteriotherapy to Treat Staphylococcus aureus in Patients With Atopic Dermatitis: A Randomized Double-blind Clinical Trial [e-pub ahead of print]. JAMA Dermatol. 2021b;157(8):978-82. doi: 10.1001/jamadermatol.2021.1311 (accessed 10 January 2022).

Nath S, Kumari N, Bandyopadhyay D, et al. Dysbiotic Lesional Microbiome With Filaggrin Missense Variants Associate With Atopic Dermatitis in India. Front Cell Infect Microbiol. 2020;10:570423.

Oetjen LK, Mack MR, Feng J, et al. Sensory Neurons Co-opt Classical Immune Signaling Pathways to Mediate Chronic Itch. Cell. 2017;171(1):217-228.e13.

Queck SY, Jameson-Lee M, Villaruz AE, et al. RNAIII-independent target gene control by the agr quorum-sensing system: insight into the evolution of virulence regulation in Staphylococcus aureus. Mol Cell. 2008;32(1):150-8.

Park HY, Kim CR, Huh IS, et al. Staphylococcus aureus Colonization in Acute and Chronic Skin Lesions of Patients with Atopic Dermatitis. Ann Dermatol. 2013;25(4):410-6.

Reich K, Teixeira HD, de Bruin-Weller M, et al. Safety and efficacy of upadacitinib in combination with topical corticosteroids in adolescents and adults with moderate-to-severe atopic dermatitis (AD Up): results from a randomised, double-blind, placebo-controlled, phase 3 trial. Lancet. 2021;397(10290):2169-81.

Sawada Y, Tong Y, Barangi M, et al. Dilute bleach baths used for treatment of atopic dermatitis are

not antimicrobial in vitro. J Allergy Clin Immunol. 2019;143(5):1946-48

Schoeberl B. Quantitative Systems Pharmacology models as a key to translational medicine. Curr Opin Syst Biol 2019;16:25–31

Schram ME, Spuls PI, Leeflang MM, Lindeboom R, Bos JD, Schmitt J. EASI, (objective) SCORAD and POEM for atopic eczema: responsiveness and minimal clinically important difference. Allergy. 2012;67:99-106

Schröder JM. Antimicrobial peptides in healthy skin and atopic dermatitis. Allergol Int. 2011;60(1):17-24

Seltmann J, Roesner LM, von Hesler FW, Wittmann M, Werfel T. IL-33 impacts on the skin barrier by downregulating the expression of filaggrin. J Allergy Clin Immunol. 2015;135(6):1659-61.e4

Shah DK, Betts AM. Antibody biodistribution coefficients: inferring tissue concentrations of monoclonal antibodies based on the plasma concentrations in several preclinical species and human. MAbs. 2013;5(2):297-305

Sieprawska-Lupa M, Mydel P, Krawczyk K, et al. Degradation of human antimicrobial peptide LL-37 by Staphylococcus aureus-derived proteinases. Antimicrob Agents Chemother. 2004;48(12):4673-9.

Sihto HM, Stephan R, Engl C, Chen J, Johler S. Effect of food-related stress conditions and loss of agr and sigB on seb promoter activity in S. aureus. Food Microbiol. 2017;65:205-12.

Silverberg JI, Toth D, Bieber T, et al. Tralokinumab plus topical corticosteroids for the treatment of moderate-to-severe atopic dermatitis: results from the double-blind, randomized, multicentre, placebo-controlled phase III ECZTRA 3 trial. Br J Dermatol. 2021;184(3):450-63.

Simpson EL, Bieber T, Eckert L, Wu R, Ardeleanu M, Graham NM, Pirozzi G, Mastey V. Patient burden of moderate to severe atopic dermatitis (AD): Insights from a phase 2b clinical trial of dupilumab in adults. J Am Acad Dermatol. 2016a;74:491-8

Simpson EL, Bieber T, Guttman-Yassky E, et al. Two Phase 3 Trials of Dupilumab versus Placebo in Atopic Dermatitis. N Engl J Med. 2016b;375:2335-48

Simpson EL, Parnes JR, She D, et al. Tezepelumab, an anti-thymic stromal lymphopoietin monoclonal antibody, in the treatment of moderate to severe atopic dermatitis: A randomized phase 2a clinical trial. J Am Acad Dermatol. 2019;80(4):1013-21

Storn R and Price K. Differential evolution–a simple and efficient heuristic for global optimization over continuous spaces. J Global Optimization. 1997;11(4), 341-59

Syed AK, Reed TJ, Clark KL, Boles BR, Kahlenberg JM. Staphlyococcus aureus phenol-soluble modulins stimulate the release of proinflammatory cytokines from keratinocytes and are required for induction of skin inflammation. Infect Immun. 2015;83(9):3428-37.

Tham EH, Koh E, Common JEA, Hwang IY. Biotherapeutic Approaches in Atopic Dermatitis. Biotechnol J. 2020;15(10):e1900322.

van Dalen R, De La Cruz Diaz JS, Rumpret M, et al. Langerhans Cells Sense Staphylococcus aureus Wall Teichoic Acid through Langerin To Induce Inflammatory Responses. mBio. 2019;10(3):e00330-19

Vazquez ML, Kaila N, Strohbach JW, et al. Identification of N-{cis-3-[Methyl(7H-pyrrolo[2,3-d]pyrimidin-4-yl)amino]cyclobutyl}propane-1-sulfonamide (PF-04965842): A Selective JAK1 Clinical Candidate for the Treatment of Autoimmune Diseases. J Med Chem. 2018;61:1130-52

Wang EB, Shen L, Heathman M, Chan JR. Incorporating Placebo Response in Quantitative Systems Pharmacology Models. CPT Pharmacometrics Syst Pharmacol. 2019;8(6):344-6

Wanner S, Schade J, Keinhörster D, et al. Wall teichoic acids mediate increased virulence in Staphylococcus aureus. Nat Microbiol. 2017;2:16257.

Williams MR, Costa SK, Zaramela LS, et al. Quorum sensing between bacterial species on the skin protects against epidermal injury in atopic dermatitis. Sci Transl Med. 2019;11(490):eaat8329.

Wong SM, Ng TG, Baba R. Efficacy and safety of sodium hypochlorite (bleach) baths in patients with moderate to severe atopic dermatitis in Malaysia. J Dermatol. 2013;40(11):874-80.

Yamaguchi M, Sayama K, Yano K, et al. IgE enhances Fc epsilon receptor I expression and IgE-dependent release of histamine and lipid mediators from human umbilical cord blood-derived mast cells: synergistic effect of IL-4 and IgE on human mast cell Fc epsilon receptor I expression and mediator release. J Immunol. 1999;162(9):5455-65

TABLE and FIGURES

TABLE 1 Treatments considered in this study

Treatments	Targets	Dose regimen (highest dose)	Reported efficacies	#patients in placebo/treatment group (Phase)
S. hominis A9 (*Sh*A9) (Nakatsuji et al., 2021a)	Microbes	2 g (to deliver 1×10^6 CFU/cm^2) twice/day, topical, for 1 week (follow-up until 10 days).	%improved local EASI† *S. aureus*	17/35 (Ph1). Of 35, 21 and 11 patients were colonised with *S. aureus* that is sensitive and resistant to *Sh*A9 bacteriocin, respectively. Colonisation status of the remaining 3 patients were not determined.
Flucloxacillin (Ewing et al., 1998)	Microbes	250 mg 4 times/day, oral, for 4 weeks (follow-up until 12 weeks).	Surface area score‡ Erythema score‡ *S. aureus*	25/25 (Ph2)
Dupilumab (anti-IL-4 receptor subunit α antibody) (Callewaert et al., 2020; 34. Blauvelt et al., 2017; Guttman-Yassky et al., 2019a)	IL-4 and IL-13	400 mg followed by 200 mg weekly, subcutaneous	EASI-75 %improved EASI *S. aureus*	27/27 (Ph2)
		600 mg followed by 300 mg, weekly, subcutaneous, with concomitant use of topical corticosteroids	EASI-75, %improved EASI	264/270 (Ph3)

†: We used %improved local EASI for %improved EASI as *Sh*A9 was applied on the ventral forearms locally,

‡: We regarded %improved score of a product of the surface area score and the erythema score as %improved EASI by assuming that the erythema represents the four signs (erythema, induration, excoriations and lichenification) for the EASI score, which is calculated as a product of the area score and the severity score of the four signs. For dupilumab, we adopted *S. aureus* levels in Ph2 study and %improved EASI and EASI-75 in Ph3 study (SI Section 1).

FIGURE 1 Three treatments (flucloxacillin, *Sh*A9 and dupilumab) reduced *S. aureus* levels but demonstrated conflicting clinical efficacies regarding EASI scores. *S. aureus* levels, the EASI score and EASI-75 were normalised using the reported data of each clinical trial (SI Section 2). For *Sh*A9, we evaluated the efficacies for the patients stratified by whether the colonised *S. aureus* is sensitive to *Sh*A9 bacteriocins (*Sh*A9-sensitive) or is resistant to *Sh*A9 bacteriocins (*Sh*A9-resistant). Horizontal bars on top represent the dosing periods in each clinical trial. Error bars: standard deviation.

FIGURE 2 Overview of the QSP model that describes the interactions between *S. aureus* and CoNS in AD pathogenesis. (a) Schematic diagram. (b) Regulatory pathways of the QSP model. The model comprises of the EASI score (an efficacy endpoint), skin barrier integrity, agr expression, *S. aureus*, CoNS, IL-4/IL-13 and treatments (*Sh*A9, flucloxacillin and dupilumab). The regulatory pathways between biological factors are described according to published human data (SI Section 3).

FIGURE 3 QSP model-based simulation reproduced the reference data. The distributions of the model parameters were optimised to minimize the difference between simulated and reference data (SI Section 4). Simulation was conducted on 1000 virtual patients. **(a)** Comparison of baseline levels of biological factors between reference (striped bars) and simulated data (filled bars). Error bars: standard deviation. **(b)** Comparison of clinical efficacies of flucloxacillin, *Sh*A9 and dupilumab between reference (unfilled circles: mean. error bars: standard deviation) and simulated (lines: mean. shaded area: standard deviation.) data**. (c)** Simulated model variables that have no reference data (lines: mean. shaded area: standard deviation.). The IL-4/IL-13 levels in dupilumab reflect the 99% inhibition of IL-4/IL-13 by dupilumab. Green lines represent dosing periods. Effects of *Sh*A9 were applied in both dosing and follow-up periods in the simulation because the measured amounts of *Sh*A9 on the skin remained higher than baseline levels during the follow-up periods in the actual clinical trial (Nakatsuji et al., 2021a), while effects of flucloxacillin and dupilumab were applied only during dosing periods.

FIGURE 4 Detrimental effects of flucloxacillin and *Sh*A9 on EASI scores disappeared if their bactericidal activity against CoNS were hypothetically removed. The EASI scores and EASI-75 of flucloxacillin and *Sh*A9 (yellow, red and purple solid lines) were compared with hypothetical situation where flucloxacillin and *Sh*A9 have no bactericidal effects on CoNS (yellow, red and purple dashed lines). The efficacies of dupilumab (blue solid line), the effects of which were modelled by inhibiting IL-4/IL-13 by 99%, were shown as a reference. Simulation was conducted on 1000 virtual patients (The EASI scores: mean values. EASI-75: responder rates). Without bactericidal effects on CoNS, flucloxacillin and *Sh*A9 achieved better efficacies than placebo (black thin line) in our simulation. The simulation of efficacies of *Sh*A9 was stopped on day 10 because our model was calibrated to reproduce the reported efficacies of *Sh*A9 until day 10.

FIGURE 5 Hypothetical *S. aureus*-targeted therapies achieved better EASI-75 after 16 weeks of treatment than dupilumab in our model simulation. (a) Antimicrobial effects of hypothetical *S. aureus*-targeted therapies are represented by the level of *S. aureus*, that of CoNS and the inhibition level of agr expression after 16 weeks of treatment. Hypothetical *S. aureus*-targeted therapies were represented in our model by varying strengths of *S. aureus* killing, CoNS killing and inhibition of agr expression. (b and c) Antimicrobial effects of hypothetical *S. aureus*-targeted therapies evaluated by EASI-75 after 16 weeks of treatment for all virtual patients (b) and for virtual dupilumab poor responders (c). Lower *S. aureus* levels, higher CoNS levels and stronger inhibition of agr expression achieved a better EASI-75. The hypothetical *S. aureus*-specific eradication (yellow arrows) achieved comparable (b) or better (c) EASI-75 to dupilumab (dotted line in (b) and 0% in (c)), and its EASI-75 was potentiated

(triangle) by adding 90% inhibition of agr expression (blue arrows). Their combination application with dupilumab achieved better EASI-75 than an application of either one. The effects of dupilumab were modelled by inhibiting IL-4/IL-13 by 99%. Simulation was conducted on 1000 virtual patients or 1000 virtual dupilumab poor responders (levels of *S. aureus* and CoNS and the inhibition level of agr expression: mean values. EASI-75: responder rates).

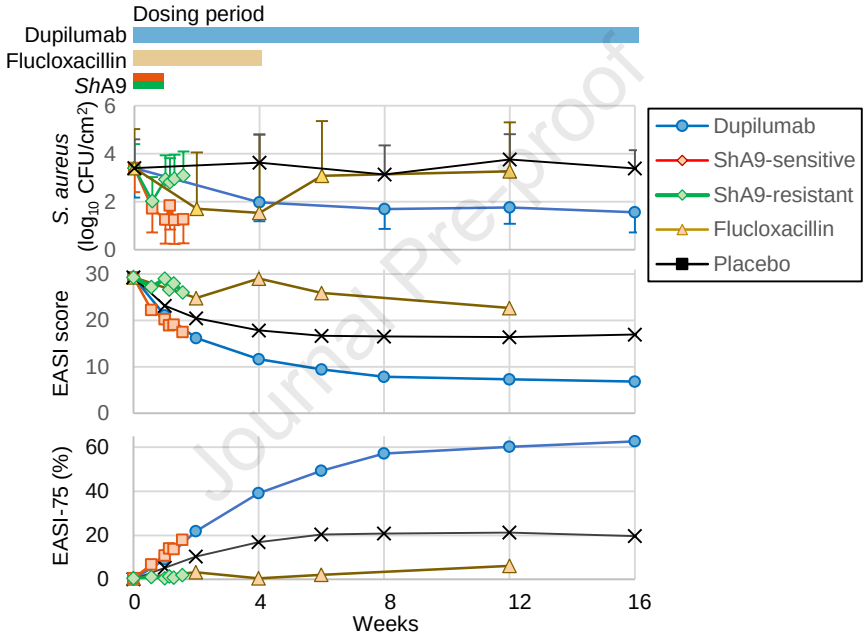

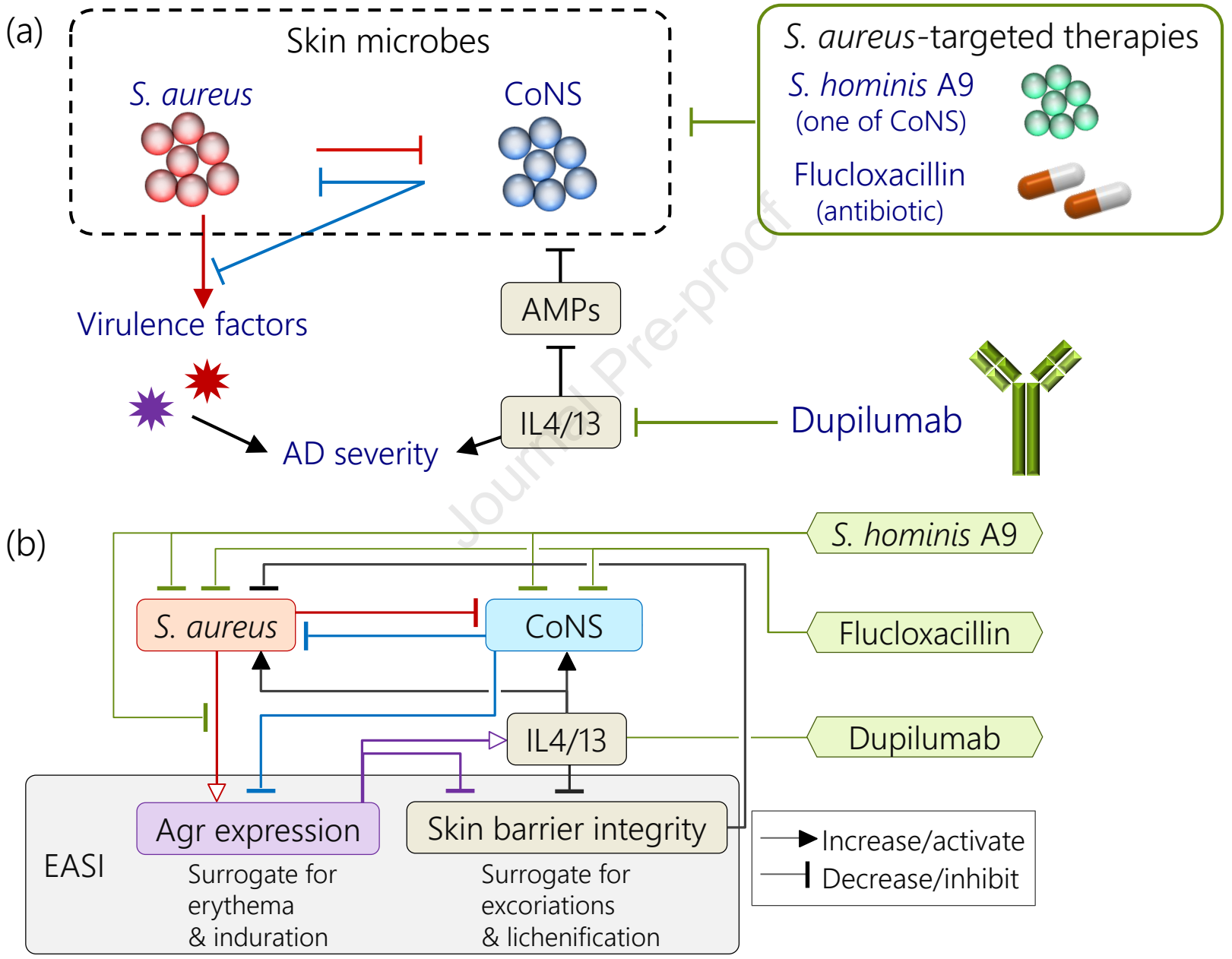

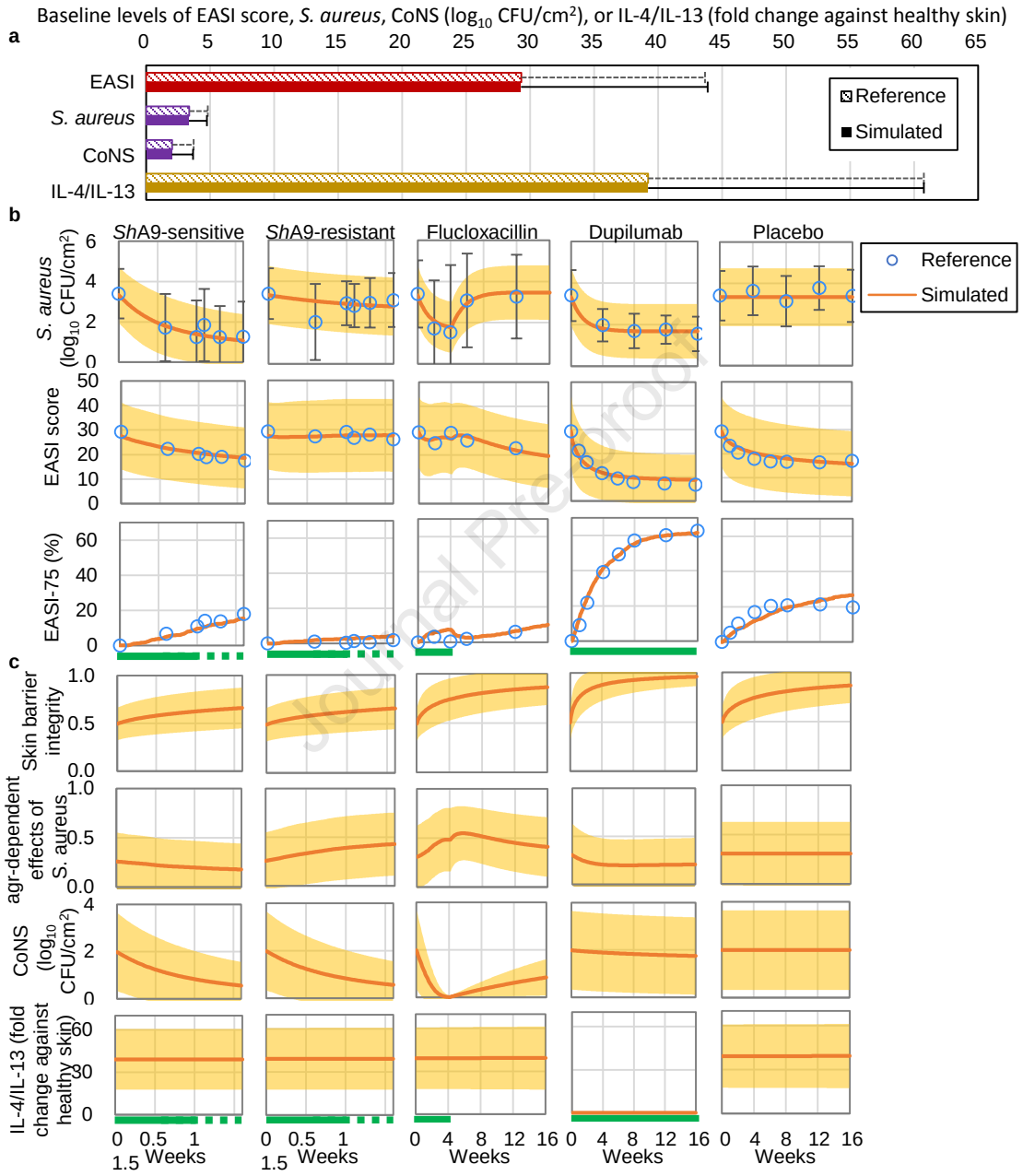

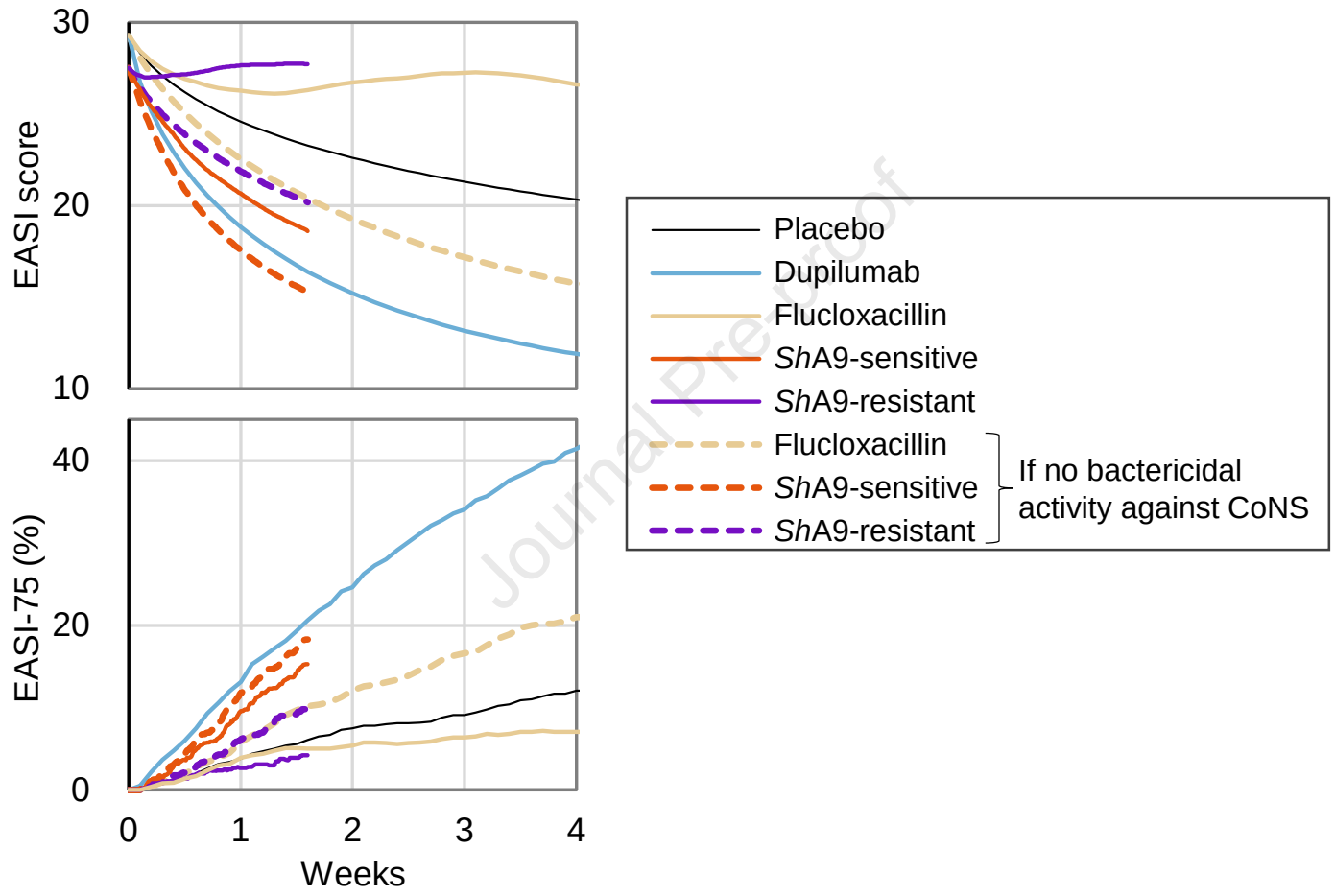

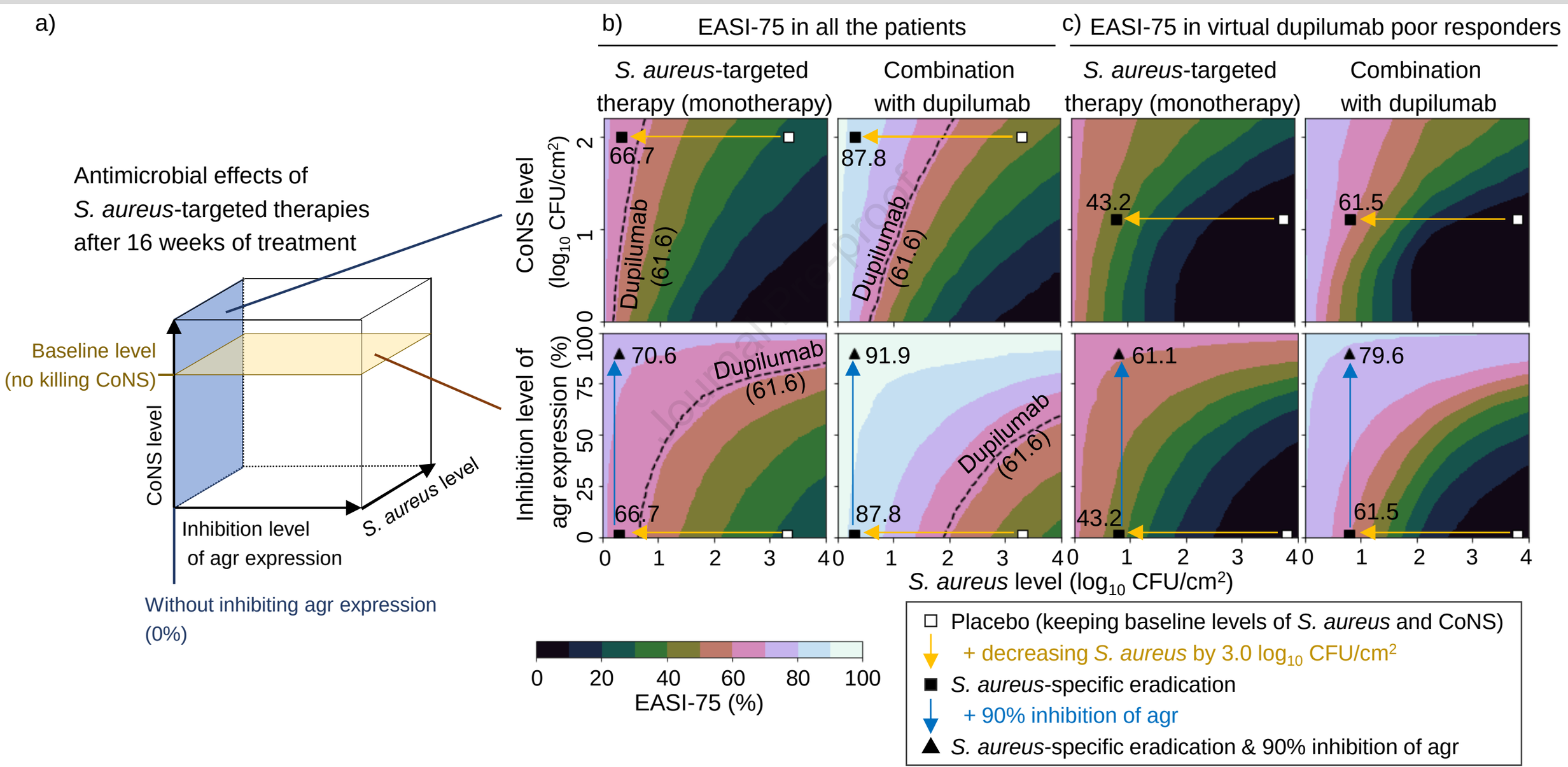

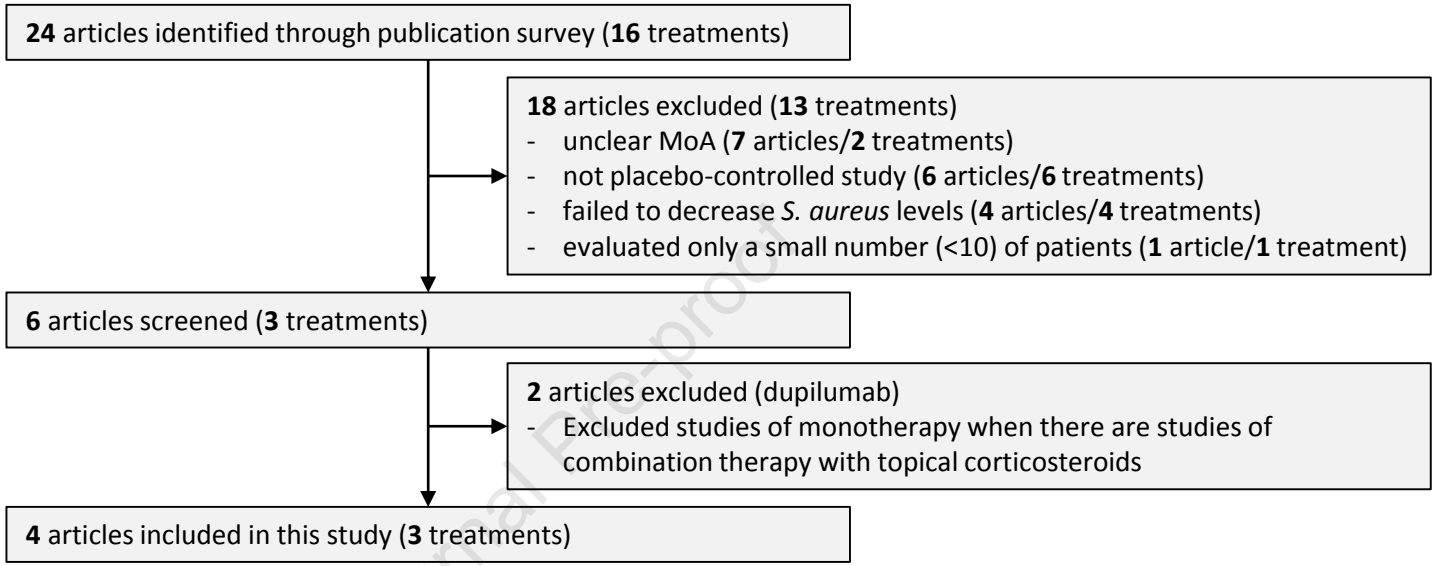

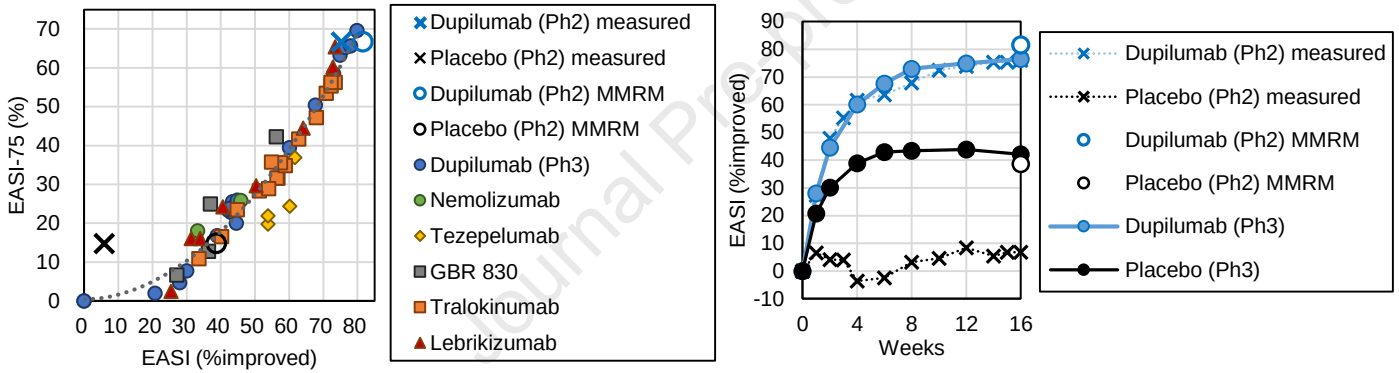

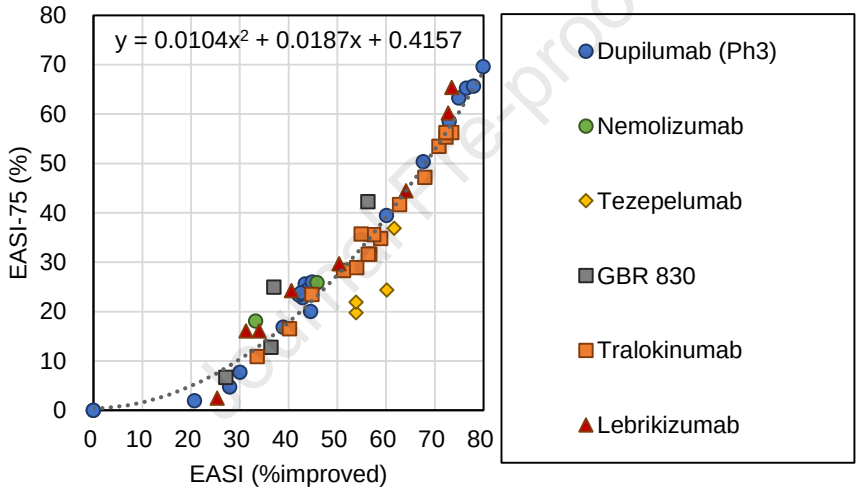

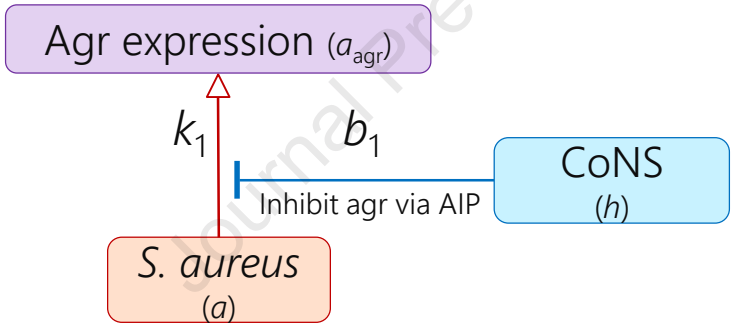

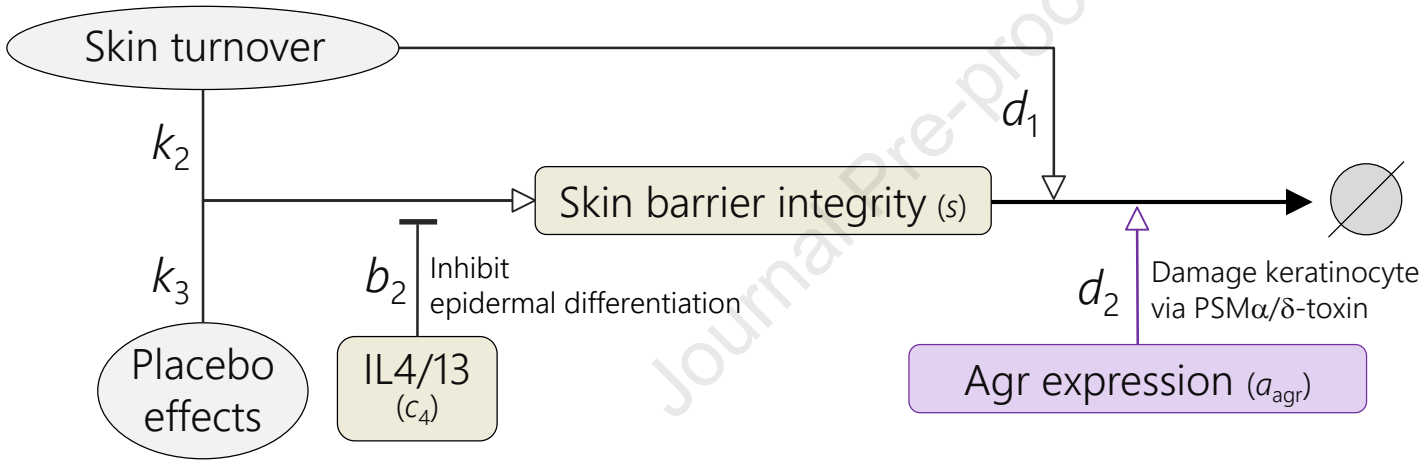

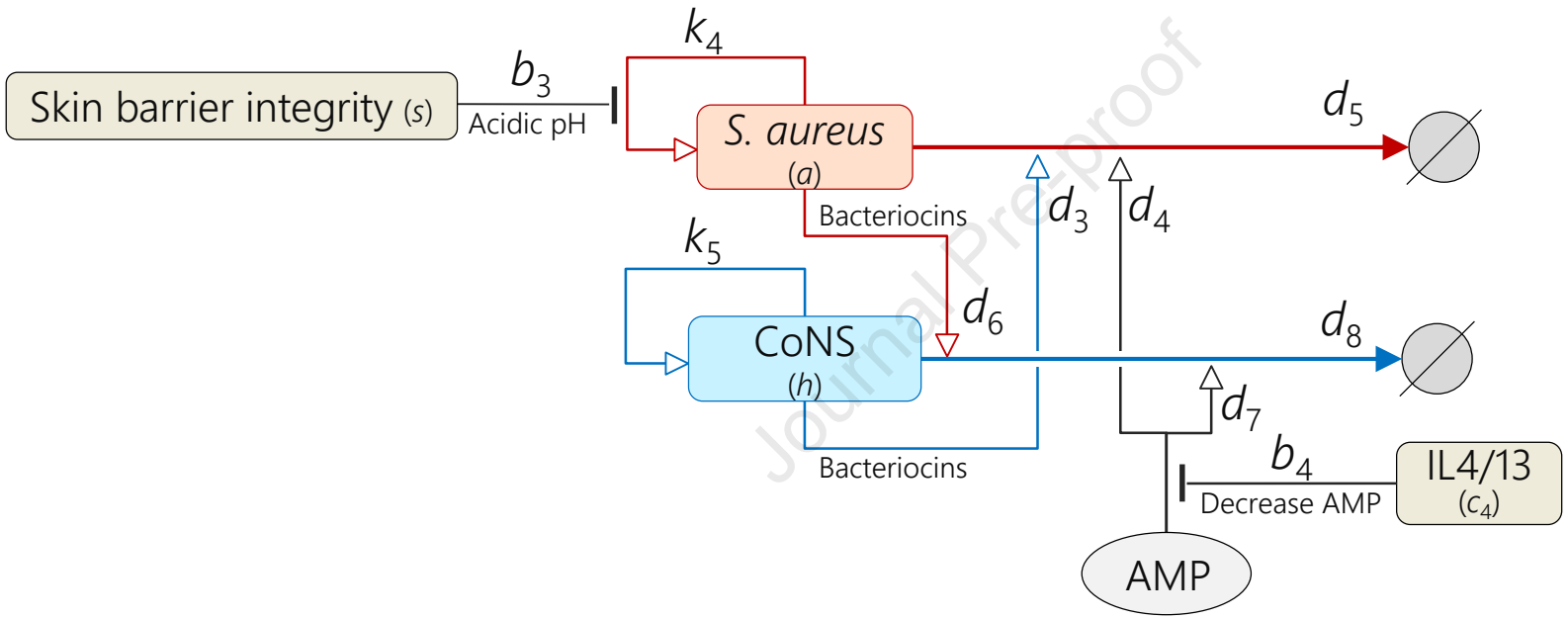

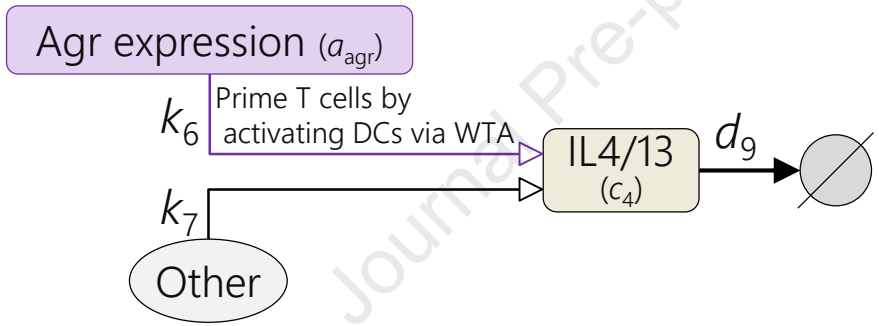

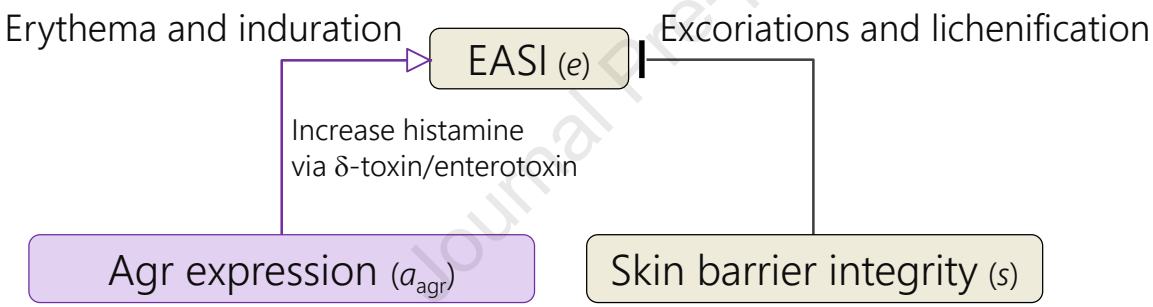

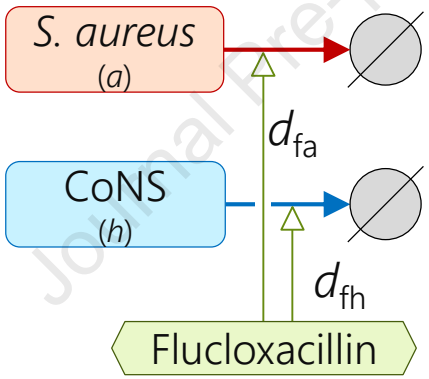

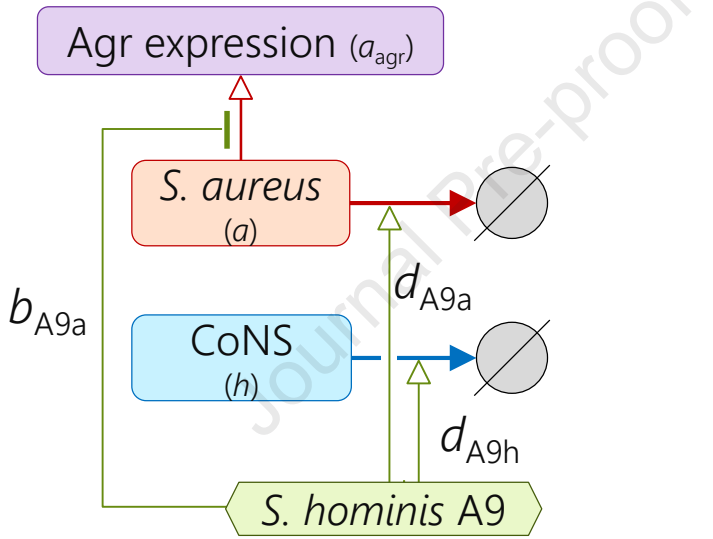

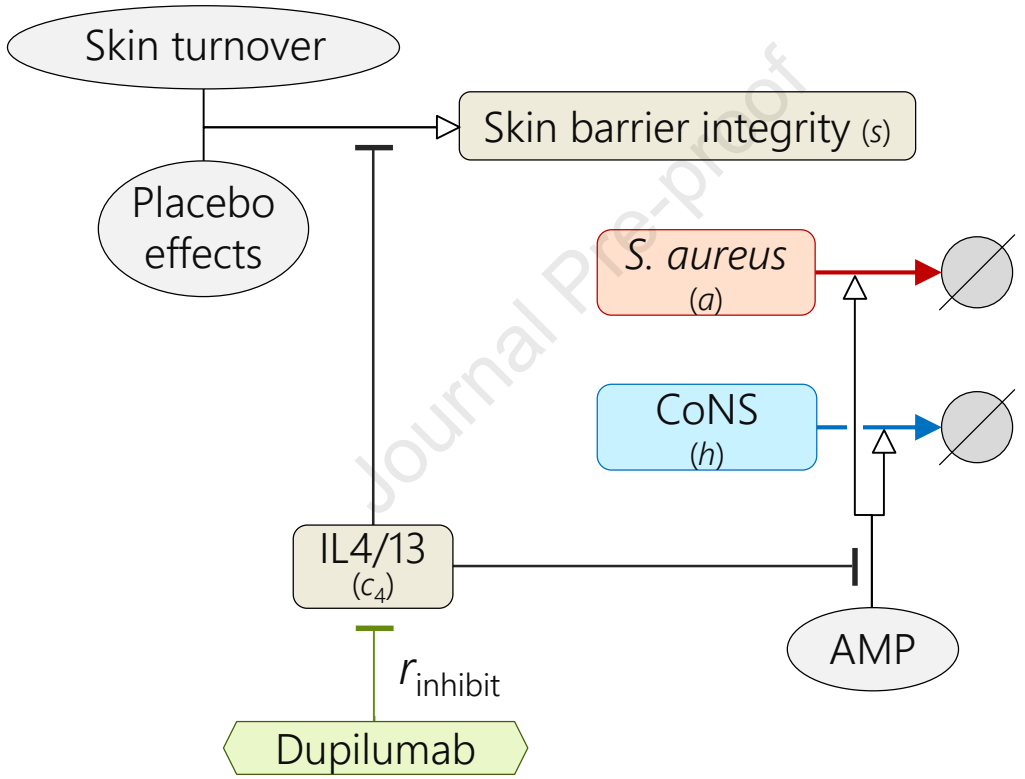

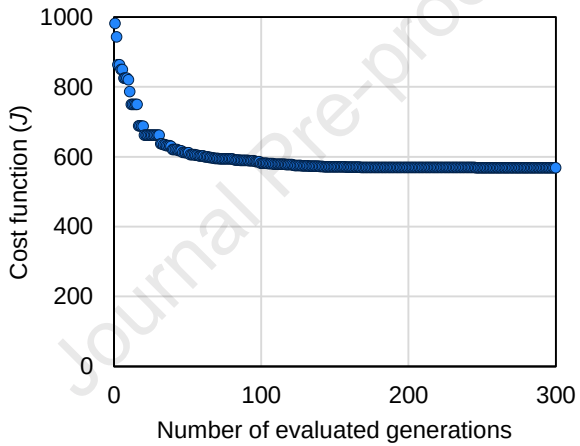

Parameters		%improved EASI				
		Placebo	Dupilumab	*Sh* A9-sensitive	*Sh* A9-resistant	Flucloxacillin
Strength of agr expression of *S. aureus*	k1	-0.3	-0.2	0.0	-0.1	-0.1
Recovery rate of skin barrier integrity via skin turnover	k2	0.0	0.0	0.0	0.0	0.0
Recovery rate of skin barrier integrity via placebo effects	k3	0.5	0.1	0.4	0.2	0.3
Proliferation rate of *S. aureus*	k4	-0.5	-0.7	-0.3	-0.4	-0.6
Proliferation rate of CoNS	k5	0.5	0.4	-0.2	-0.1	-0.3
Secretion rate of IL-4/IL-13 via agr expression	k6	0.0	0.0	0.0	0.0	0.0
Secretion rate of IL-4/IL-13 via other pathways	k7	-0.1	0.0	0.0	0.0	0.0
Inhibitory strength for agr expression via CoNS	b1	0.2	0.1	-0.1	-0.1	-0.1
Inhibitory strength for recovery of skin barrier via IL-4/IL-13	b2	-0.4	0.0	-0.3	-0.2	-0.2
Inhibitory strength for *S. aureus* proliferation via skin barrier	b3	0.0	0.0	0.0	0.0	-0.1
Inhibitory strength for elimination of Staphylococci via IL-4/IL-13	b4	-0.1	0.0	0.0	0.0	-0.1
Degradation rate of skin barrier via skin turnover	d1	0.0	0.0	0.0	0.1	0.0
Degradation rate of skin barrier via *S. aureus*	d2	0.0	0.0	0.0	0.0	0.1
Killing rate of *S. aureus* via bacteriocins secreted from CoNS	d3	0.0	0.0	0.0	0.0	0.0
Killing rate of *S. aureus* via AMPs	d4	0.1	0.5	0.0	0.1	0.1
Elimination rate of *S. aureus* via turnover	d5	0.4	0.3	0.0	0.2	0.2
Killing rate of CoNS via bacteriocins secreted from *S. aureus*	d6	0.0	0.0	-0.1	0.0	0.0
Killing rate of CoNS via AMPs	d7	-0.1	-0.1	0.1	0.1	0.0
Elimination rate of CoNS via turnover	d8	-0.5	-0.4	0.2	0.2	0.3
Elimination rate of IL-4/IL-13	d9	0.1	0.0	0.1	0.1	0.1
Killing rate of *S. aureus* via *Sh* A9 in bacteriocin-sensitive *S. aureus*	dA9a_s	0.0	0.0	0.4	0.0	-0.1
Killing rate of *S. aureus* via *Sh* A9 in bacteriocin-resistant *S. aureus*	dA9a_r	0.0	0.0	0.0	0.1	0.0
Killing rate of CoNS via ShA9	dA9h	0.0	0.0	-0.3	-0.4	-0.1
Inhibitory strength for agr expression of *S. aureus* via *Sh* A9	bA9s	0.0	0.0	0.0	0.1	0.0
Killing rate of *S. aureus* via flucloxacillin	dfa	0.0	0.0	0.0	0.0	0.3
Killing rate of CoNS via flucloxacillin	dfh	0.0	0.0	0.0	0.0	-0.3

SUPPLEMENTARY INFORMATION

1. Selection of clinical studies for development of the QSP model

We used pre-defined inclusion and exclusion criteria (FIGURE S) to select clinical studies to be referenced in development of the QSP model. Firstly, we identified 24 clinical trials that reported both *S. aureus* levels and AD severity scores in a placebo-controlled study. We then excluded 18 clinical trials as the treatments have unclear MoA, they failed to decrease *S. aureus* levels compared to placebo, or they evaluated only a small number (<10) of patients. TABLE S3 lists the treatments excluded in this study. As for antibiotics/antiseptics, 23 clinical trials were investigated in Cochrane review (George et al., 2019), from which we included only one study (Ewing et al., 1998) with flucloxacillin which met our inclusion criteria.

As for dupilumab, we included the data of *S. aureus* levels in Ph2 study (Callewaert et al., 2020) and %improved EASI and EASI-75 in Ph3 study (Blauvelt et al., 2017). Detailed rationale for this choice is as follows.

1) %improved EASI and EASI-75 were reported in both Ph2 and Ph3 studies. However, *S. aureus* levels were reported only in Ph2 study (Callewaert et al., 2020).
2) The measured %improved EASI of placebo treatment in the Ph2 study (Callewaert et al., 2020) is not deemed to be reliable because the relationship between measured %improved EASI and EASI-75 at week 16 deviates from those in other clinical trials (FIGURE S left).
3) The estimated %improved EASI by mixed-effect model repeated measure (MMRM), which is a popular method to handling missing data (e.g., due to drop-out of patients during a clinical study) (Lane, 2008), in the Ph2 study (Callewaert et al., 2020) is deemed to be reliable because the relationship between the estimated %improved EASI and EASI-75 at week 16 in the Ph2 study (Callewaert et al., 2020) is consistent with those in other clinical trials (FIGURE S left). However, the estimated value is not time-course data (reported week 16 only) and cannot be used for our model fitting.
4) We decided to use a Ph3 study (Blauvelt et al., 2017) that reported time-course data of %improved EASI and EASI-75, because (a) the %improved EASI at week 16 in the Ph3 study (Blauvelt et al., 2017) is comparable to the estimated %improved EASI by MMRM at week 16 in the Ph2 study (Callewaert et al., 2020) (FIGURE S right, open and closed circles) and (b) time-course data of %improved EASI of dupilumab treatment in Ph2 were comparable to those in Ph3 (FIGURE S right, blue crosses and filled circles) suggesting that time-course data of %improved EASI of placebo treatment in Ph2, if they were estimated by MMRM, are comparable to those in Ph3.
5) Among several Ph3 studies for dupilumab (Blauvelt et al., 2017; Simpson et al., 2016b),

we selected a Ph3 study which used a combination therapy with topical corticosteroids (Blauvelt et al., 2017), as it is more reflective of the likely clinical use than monotherapy.

2. Data processing

We used clinical efficacies (*S. aureus* levels, %improved EASI, EASI scores and EASI-75) of flucloxacillin, *Sh*A9 and dupilumab as the reference data. The clinical efficacies were normalised to compare data from different clinical trials.

2.1. Normalisation of *S. aureus* levels

Time courses of *S. aureus* levels were reported in clinical trials of flucloxacillin (Ewing et al., 1998), *Sh*A9 (Nakatsuji et al., 2021a) and dupilumab (Callewaert et al., 2020). We described the normalised *S. aureus* level, $a_j(t)$, for the *j*-th treatment at time *t* by

$$a_j(t) = (\Delta a_j^*(t) - \Delta a_{\mathrm{P}_j}^*(t)) + \Delta a_{\mathrm{P_d}}^*(t) + a_{\mathrm{ShA9}}^*(0), \quad \text{(S1)}$$

where the first term corresponds to the net effects of the treatment defined by the difference of the change in *S. aureus* levels ($\log_{10}$ scale) at time *t* from baseline, between the *j*-th treatment ($\Delta a_j^*(t)$) and the corresponding placebo groups ($\Delta a_{\mathrm{P}_j}^*(t)$). This term adjusts for different placebo effects across clinical studies that may differ in the study participants' background, concomitant drugs and the study sites (Wang et al., 2019). The remaining two terms describe the change in *S. aureus* levels at time *t* from baseline, $\Delta a_{\mathrm{P_d}}^*(t)$, in the placebo group in the dupilumab clinical trial that evaluated efficacies for the longest period among the trials evaluated in this study and the baseline level of *S. aureus,* $a_{\mathrm{ShA9}}^*(0)$, in the *Sh*A9 clinical trial that is the only one reporting levels of both *S. aureus* and CoNS among the trials evaluated in this study.

2.2. Conversion of reported AD severity scores to %improved EASI

%improved EASI for flucloxacillin and *Sh*A9 were estimated as follows.

For flucloxacillin, we substituted %improved EASI by the %improved score of a product of the area score and the severity score of erythema (Ewing et al., 1998) (the only disease sign evaluated in that study) by assuming that the erythema represents the four disease signs (erythema, induration, excoriations and lichenification) for EASI score, which is calculated as a product of the area score and the severity score of the four signs.

For *Sh*A9, we substituted %improved EASI by the %improved local EASI of the ventral arms as *Sh*A9 was applied on the ventral forearms locally (Nakatsuji et al., 2021a).

2.3. Normalisation of %improved EASI, EASI score and EASI-75

%improved EASI, EASI score and EASI-75 were normalised in the same way as in the published paper on the QSP model of biologics (Miyano et al., 2021). We described normalised %improved EASI, $m_j(t)$, for the *j*-th treatment at *t* by

$$m_j(t) = (m_j^*(t) - m_{\mathrm{P}_j}^*(t)) + m_{\mathrm{P_d}}^*(t), \quad \text{(S2)}$$

where the first term corresponds to the net effects of the treatment defined by the difference of the efficacy (%improved EASI) between the *j*-th treatment ($m_j^*(t)$) and the corresponding placebo groups ($m_{\mathrm{P}_j}^*(t)$). This term adjusts for different efficacies in the placebo group across the clinical studies due to differences in study participants' background, concomitant drugs and sites of study (Wang et al., 2019). The second term corresponds to the placebo effects defined by the efficacy in the placebo group in the dupilumab clinical trial ($m_{\mathrm{P_d}}^*(t)$).

Normalised mean EASI score, $e_j(t)$, of the *j*-th treatment at *t* was calculated by

$$e_j(t) = \frac{e_{\mathrm{d}}(0)(100 - m_j(t))}{100}, \quad \text{(S3)}$$

where $e_{\mathrm{d}}(0)$ is the reported baseline (before the trial) mean EASI score in the dupilumab clinical trial (Blauvelt et al., 2017) and $m_j(t)$ is the normalised %improved EASI defined in (S2).

Normalised EASI-75 was estimated from the normalised %improved EASI using a regression curve obtained from the relationship between %improved EASI and EASI-75 in clinical trials of multiple treatments (Blauvelt et al., 2017 Kabashima et al., 2020; Simpson et al., 2019; Guttman-Yassky et al., 2019a; Guttman-Yassky et al., 2020; Silverberg et al., 2021) (FIGURE S).

3. Model structure

The QSP model of *S. aureus*-targeted therapies (FIGURE 2) describes the dynamics of EASI score, skin barrier integrity, *S. aureus*, CoNS, IL-4/IL-13 and treatment effects. Those dynamics were formulated by Eqs. (S4)-(S22) with six variables (TABLE S1) and 26 parameters (TABLE S2). This section introduces the equations.

t is the time after the start of treatments. The baseline levels of biological factors for our model (at *t*=0) were obtained from the simulated steady-state level (after 1000 weeks) without any intervention. We referred to the reported levels of biological factors without interventions of

the treatments as the reference values for the baseline levels, assuming that the levels of the biological factors were stable before the start of treatments.

3.1. Biological factors

(a) Agr expression level

Agr expression level, $a_{\mathrm{agr}}(t)$, of *S. aureus* is described (FIGURE S) by

$$a_{\mathrm{agr}}(t) = \tanh \frac{k_1 a(t)}{1+b_1 h(t)}, \quad \text{(S4)}$$

where $a(t)$ and $h(t)$ are *S. aureus* level and CoNS level ($\log_{10}$ CFU/cm^2), respectively and b_1 describes the inhibitory strength for the agr expression by AIPs from CoNS (Williams et al., 2019).

(b) Skin barrier integrity

The dynamics of the skin barrier integrity, $s(t)$, is described (FIGURE S4 Agr expression is regulated by *S. aureus* and CoNS

FIGURE S) by

$$\frac{ds(t)}{dt} = \frac{(1-s(t))(k_2+k_3)}{1+b_2 c_4(t)} - s(t)\{d_1 + d_2 a_{\mathrm{agr}}(t)\}, \quad \text{(S5)}$$

where $c_4(t)$ is IL-4/IL-13 level, $s(t)$ is skin barrier integrity, k_2 and k_3 describe the recovery rate of skin barrier integrity via skin turnover and that via placebo effects, respectively, b_2 describes the inhibitory strength for recovery of skin barrier via IL-4/IL-13 and d_1 and d_2 describe the degradation rate of skin barrier via skin turnover and that via *S. aureus*, respectively.

The first term represents a recovery of skin barrier integrity by intrinsic skin turnover (with the recovery rate, k_2) and placebo effects (k_3). We assumed the maximal value of $s(t) = 1$ as a healthy state of skin barrier integrity (TABLE S2), and thus modified the recovery rate by $1 - s(t)$. The placebo effect was applied to the simulations for both placebo- and drug-treated groups, as placebo-treated patients improved the EASI score (Callewaert et al., 2020; Blauvelt et al., 2017; Nakatsuji et al.,2021a), presumably because of the controlled care with

concomitant drugs such as emollients during the clinical trials. The recovery of skin barrier integrity was assumed to be compromised by IL-4 and IL-13 (with the strength b_2) as they are shown to decrease filaggrin production (Howell et al., 2009; Seltmann et al., 2015) and thereby inhibiting epidermal differentiation and as they induce pruritus (Oetjen et al., 2017) and thus scratching of skin.

The second term corresponds to the degradation of the skin barrier by skin turnover (with the degradation rate, d_1) and by *S. aureus,* which damages keratinocytes through phenol-soluble modulin-α (PSMα) and δ-toxin (d_2) (Syed et al., 2015). The latter (d_2) is agr-dependent because the agr regulates secretion of PSMα and δ-toxin from *S. aureus* (Queck et al., 2008).

(c) *S. aureus* and CoNS in the skin

The dynamics of *S. aureus* and CoNS in the skin, $a(t)$ and $h(t)$, are described (FIGURE S) by

$$\frac{da(t)}{dt} = \frac{k_4}{1+b_3 s(t)}\left(1 - \frac{a(t)}{a_{\max}}\right) - \left\{d_3 h(t) + \frac{d_4}{1+b_4 c_4(t)} + d_5\right\} \text{ and} \quad \text{(S6)}$$

$$\frac{dh(t)}{dt} = k_5\left(1 - \frac{h(t)}{h_{\max}}\right) - \left\{d_6 a(t) + \frac{d_7}{1+b_4 c_4(t)} + d_8\right\}, \quad \text{(S7)}$$

where k_4 and k_5 are the proliferation rates of *S. aureus* and CoNS, respectively, b_3 is the inhibitory coefficient for *S. aureus* proliferation via skin barrier, b_4 is the inhibitory strength for elimination of Staphylococci via IL-4/IL-13, d_3 and d_4 are the killing rate of *S. aureus* via bacteriocins secreted from CoNS and that via AMPs, respectively, d_5 is the elimination rate of *S. aureus* via turnover, d_6 and d_7 are the killing rate of CoNS via bacteriocins secreted from *S. aureus* and that via AMPs, respectively, d_8 is the elimination rate of CoNS via turnover and $a_{\max}$ and $h_{\max}$ are the maximal levels of *S. aureus* and CoNS, respectively. Eqs. (S6 and S7) represent logistic growth of $a(t)$ and $h(t)$ in $\log_{10}$ scale. We set $[a_{\max}, h_{\max}] = [7, 7]$ to cover the reported range of *S. aureus* levels (reported maximal $\log_{10}$ level of *S. aureus* was 6) in the dupilumab clinical trial (Callewaert et al., 2020).

The Eqs. (S6 and S7) are relative growth rates based on $\log_{10}$ scale ($\log_{10}$ CFU/cm^2). Their absolute growth rates can be described as

$$a^*(t) = 10^{a(t)} \quad \text{(S8)}$$

$$h^*(t) = 10^{h(t)} \quad \text{(S9)}$$

$$\frac{da^*(t)}{dt} = \frac{da(t)}{dt} a^*(t) \ln 10$$

$$= \frac{k_4}{1+b_3 s(t)}\left(1 - \frac{\log_{10} a^*(t)}{a_{\max}}\right) a^*(t) \ln 10 - \left\{d_3 \log_{10} h^*(t) + \frac{d_4}{1+b_4 c_4(t)} + d_5\right\} a^*(t) \ln 10 \quad \text{(S10)}$$

$$\frac{dh^*(t)}{dt} = \frac{dh(t)}{dt} h^*(t) \ln 10$$

$$= k_5\left(1 - \frac{\log_{10} h^*(t)}{h_{\max}}\right) h^*(t) \ln 10 - \left\{d_6 \log_{10} a^*(t) + \frac{d_7}{1+b_4 c_4(t)} + d_8\right\} h^*(t) \ln 10 \quad \text{(S11)}$$

where $a^*(t)$ and $h^*(t)$ are absolute levels (CFU/cm^2) of *S. aureus* and CoNS in the skin, respectively. The first terms of Eqs. (S10 and S11) mean that we assumed that their logistic growth is based on $\log_{10}$ scale of *S. aureus* and CoNS levels.

S. aureus and CoNS proliferate (with the rates k_4 and k_5), where healthy skin barrier integrity inhibits proliferation of *S. aureus* by making skin pH acidic (with strength b_3) whereas skin pH does not affect those of CoNS (Lambers et al., 2006; Kwaszewska et al., 2014).

S. aureus and CoNS are killed by bacteriocins (released from Staphylococci) and AMP (released from keratinocytes) directly (Schröder, 2011). Bacteriocins exert antimicrobial activity against bacteria closely related to the producer strain but not against the producer strain itself (Jack et al.,1995); *S aureus* is killed by bacteriocins from CoNS (with strength d_3) (Nakatsuji et al., 2017) and AMP (d_4), and CoNS is killed by bacteriocins from *S. aureus* (d_6) (dos Santos Nascimento et al., 2005) and AMP (d_7). AMP release from keratinocytes is inhibited by IL-4 and IL-13 (Howell et al., 2006) (b_4). *S. aureus* and CoNS in the skin decrease due to their natural death (d_5 and d_8).

We did not consider influence of *S. aureus* on AMP because the experimental evidence is controversial: *S. aureus* increases AMP release from keratinocytes via pathways that are independent of the cytokines (Menzies and Kenoyer, 2005); *S. aureus* degrades AMP by aureolysin, which is a proteinase produced by *S. aureus* (Sieprawska-Lupa et al., 2004).

(d) IL-4 and IL-13

The dynamics of IL-4 and IL-13, $c_4(t)$, is described (FIGURE S) by

$$\frac{dc_4(t)}{dt} = k_6 a_{\text{agr}}(t) + k_7 - d_9 c_4(t), \quad \text{(S12)}$$

where k_6 and k_7 are the secretion rate of IL-4/IL-13 via agr expression and that via other pathways, respectively and d_9 is the elimination rate of IL-4/IL-13.

IL-4 and IL-13 are secreted from Th2 cells that are primed by dendritic cells (DCs) specifically activated by *S. aureus*-derived wall teichoic acid (WTA) (van Dalen et al., 2019) controlled by agr (Wanner et al., 2017) (with the rate k_6). There are other pathways releasing IL-4/IL-13, which were implicitly described as "other" effects (k_7).

(e) EASI score

The EASI score (ranging from 0 to 72) is calculated using the severity and the area scores of equally-weighted four AD signs (erythema, induration, excoriations and lichenification) on four body regions (head/neck, trunk, upper limbs and lower limbs) (Hanifin et al., 2001). In our model, the EASI score, $e(t)$, is described (FIGURE S) by

$$e(t) = 72\,\frac{2a_{\mathrm{agr}}(t)+2(1-s(t))}{4}, \qquad \text{(S13)}$$

where 72 is the maximal EASI score. Scores derived from two AD signs (erythema and induration) and those from the remaining two signs (excoriations and lichenification) were surrogated by $a_{\mathrm{agr}}(t)$ and $1-s(t)$, respectively, as described below. We set $e(0) = 29.3$, the baseline EASI score of the AD patients in the dupilumab clinical trial, which was used as a reference value to normalise the EASI scores in all the clinical trials.

We assumed the scores derived from erythema and induration are governed by $a_{\mathrm{agr}}(t)$ because these two signs can be induced by *S. aureus* (Leung et al., 2000). We used $\log_{10}$ level of *S. aureus* to model $a_{\mathrm{agr}}(t)$ in Eq. (S4) as the correlation between EASI score and $\log_{10}$ level of *S. aureus* has been reported (Callewaert et al., 2020). Erythema is caused by inflammatory vasodilation by histamines (Grossmann et al., 1999). Histamine is released mainly from mast cells and basophils that are activated by detecting antigens, such as δ-toxin (Azimi et al., 2017) and Staphylococcus enterotoxins (Leung et al., 1993), released by *S. aureus* but not by CoNS (Becker et al., 2001). We associated the released histamine concentration with the antigen load in this model because the amount of histamine release depends more on the amount of antigens than that of antigen-specific IgE (Yamaguchi et al., 1999), although both antigens and antigen-specific IgE play a role in this process (Amin, 2012). A negligible contribution of IgE (compared to that of antigens) on the AD pathogenesis is also suggested by a lack of clinical efficacy demonstrated for omalizumab (IgE neutralizing anti-IgE antibody). Our model assumed that the histamine release by *S. aureus*-induced δ-toxin and enterotoxins depends on the agr expression level of *S. aureus* because AIPs from other strains regulate secretion of δ-toxin and enterotoxins from *S. aureus* (Queck et al., 2008; Sihto et al., 2017). Scores for the other two AD signs, excoriations and lichenification,

are surrogated by $1 - s(t)$, which describes the degree of damage of the skin barrier integrity, because excoriations and lichenification are caused by scratching (Bohl, 2019), which damages skin barrier integrity.

3.2. Treatment effects

3.2.1. Flucloxacillin

Flucloxacillin, an antibiotic, kills the Staphylococci (*S. aureus* and CoNS). We described the effects of flucloxacillin (FIGURE S) on decreasing the Staphylococci by adding the killing rates of Staphylococci (d_{fa} and d_{fh}) in Eqs. (S6 and S7):

$$\frac{da(t)}{dt} = \frac{k_4}{1+b_3 s(t)}\left(1 - \frac{a(t)}{a_{\max}}\right) - \left\{d_4 h(t) + \frac{d_5}{1+b_4 c_4(t)} + d_6 + d_{\mathrm{fa}}\right\}, \quad \text{(S14)}$$

$$\frac{dh(t)}{dt} = k_5\left(1 - \frac{h(t)}{h_{\max}}\right) - \left\{d_6 a(t) + \frac{d_7}{1+b_4 c_4(t)} + d_8 + d_{\mathrm{fh}}\right\}. \quad \text{(S15)}$$

3.2.2. *S. hominis* A9 (*Sh*A9)

***Sh*A9 is a specific strain of *S. hominis*, which produces bacteriocins against *S. aureus* (Nakatsuji et al.,2021a) and inhibits agr expression of *S. aureus* (Williams et al., 2019). Although *Sh*A9 was screened based on selectivity of the bacteriocins against *S. aureus*, it still has antimicrobial activity against CoNS (Nakatsuji et al., 2017). We describe those effects (FIGURE S9** Effects of flucloxacillin. Squared and hexagon symbols represent model variables and a treatment in our model, respectively.

FIGURE S) by adding the killing rates of *S. aureus* and CoNS (d_{A9a} and d_{A9h}) in Eqs. (S6 and S7) and the inhibitory strength for agr expression (b_{A9a}) in Eq. (S7):

$$\frac{da(t)}{dt} = \frac{k_4}{1+b_3 s(t)}\left(1 - \frac{a(t)}{a_{\max}}\right) - \left\{d_4 h(t) + \frac{d_5}{1+b_4 c_4(t)} + d_6 + d_{\mathrm{A9a}}\right\}, \quad \text{(S16)}$$

$$\frac{dh(t)}{dt} = k_5\left(1 - \frac{h(t)}{h_{\max}}\right) - \left\{d_6 a(t) + \frac{d_7}{1+b_4 c_4(t)} + d_8 + d_{\mathrm{A9h}}\right\}, \quad \text{(S17)}$$

$$a_{\mathrm{agr}}(t) = \tanh\frac{k_1 a(t)}{(1+b_1 h(t))(1+b_{\mathrm{A9a}})}. \quad \text{(S18)}$$

The clinical trial of *Sh*A9 stratified the patients according to the sensitivity of *S. aureus* isolated from each patient to the bacteriocins of *Sh*A9. The colonised *S. aureus* was categorised as "sensitive" when minimal inhibitory concentration (MIC) of *Sh*A9 conditioned medium against *S. aureus* is less than 100% (% of original conditioned medium) and as "resistant" when the MIC is more than 200% (Nakatsuji et al., 2021a). Hereafter, *Sh*A9 applied to patients colonised with *S. aureus* that is sensitive to *Sh*A9 bacteriocins is referred as *Sh*A9-sensitive and those with *S. aureus* that is resistant to *Sh*A9 bacteriocins is referred as *Sh*A9-resistant. We modelled the different sensitivity of *S. aureus* to the bacteriocins of *Sh*A9 as

$$d_{\mathrm{A9a}} = \begin{cases} d_{\mathrm{A9a\_s}}, & \text{if } ShA9 - \text{sensitive} \\ d_{\mathrm{A9a\_r}}, & \text{if } ShA9 - \text{resistant}. \end{cases} \quad \text{(S19)}$$

Effects of *Sh*A9 were applied in both dosing and follow-up periods in the simulation because the measured amount of *Sh*A9 remained higher than baseline levels during the follow-up periods in the clinical trial (Nakatsuji et al., 2021a).

3.2.3. Dupilumab

We described the effects of dupilumab (FIGURE S9 Effects of flucloxacillin. Squared and hexagon symbols represent model variables and a treatment in our model, respectively.

FIGURE S10 Effects of *S. hominis* A9. Squared and hexagon symbols represent model variables and a treatment in our model, respectively.

FIGURE S) that inhibit the signalling of IL-4 and IL-13 by scaling the concentrations of IL-4 and IL-13. Effective concentrations of the IL-4 and IL-13 in the skin at *t*, $c_4(t)$, was modelled by

$$c_4(t) = (1 - r_{\mathrm{inhibit}})c_4^*(t), \quad \text{(S20)}$$

$$r_{\mathrm{inhibit}} = \frac{d_{\mathrm{skin}}}{\mathrm{IC}_{50} + d_{\mathrm{skin}}}, \quad \text{(S21)}$$

$$d_{\mathrm{skin}} = r_{\mathrm{skin/serum}} d_{\mathrm{serum}}, \quad \text{(S22)}$$

where $c_4^*(t)$ is the concentration of IL-4 and IL-13 in the skin at *t,* r_{inhibit} is the rate of the IL-4 and IL-13 inhibition in the dupilumab treatment, d_{skin} is the concentration of dupilumab in the skin, IC_{50} is the half-maximal inhibitory concentration of dupilumab against IL-4 and IL-13, $r_{\mathrm{skin/serum}}$ is the ratio of dupilumab concentration in the skin to that in serum and d_{serum}

is the mean concentration of the dupilumab in serum. We adopted $r_{\mathrm{skin/serum}} = 0.157$ for dupilumab based on the estimated ratio of antibody concentration in the skin to that in the plasma (Shah et al., 2013). Values of IC_{50} (IL-4: <0.01 and IL-13: 0.01 mcg/mL) and d_{serum} (183 mcg/mL) were obtained from reported results of in vitro assay and the reported pharmacokinetic data of the adopted dose regimen (TABLE 1) in clinical trials (D'Ippolito and Pisano, 2018; Le Floc'h et al., 2020). With these values, r_{inhibit} was calculated as 0.99.

4. Optimising model parameters to reproduce clinical data

We optimised 52 parameters (μ_i and σ_i) that define the distributions of the 26 model parameters (TABLE S2) so that the model reproduces the following clinical data consisting of 108 reference values;

- mean values and %CV of 4 biological factors (IL-4/IL-13, *S. aureus*, CoNS and the EASI score) without interventions of the treatments (TABLE S1; 2 indices x 4 factors = 8 reference values),
- the EASI score and EASI-75 in the clinical trials (FIGURE 1; 2 indices x 5 interventions x 4-7 time points/intervention = 56 reference values) and
- mean values and %CV of *S. aureus* levels in the clinical trials (FIGURE 1; 2 indices x 5 interventions x 4-5 time points/intervention = 44 reference values).

We searched the parameters that minimize the cost function, *J*, defined by

$$J = w_1 J_1 + w_2 J_2 + w_3 J_3 + w_4 J_4 + w_5 J_5 + w_6 J_6, \tag{S23}$$

where

$$J_1 = \sqrt{\frac{1}{4}\sum_{l=1}^{4}\left(b_{\mathrm{mean},l} - \hat{b}_{\mathrm{mean},l}\right)^2}, \tag{S24}$$

$$J_2 = \sqrt{\frac{1}{4}\sum_{l=1}^{4}\left(b_{\mathrm{CV},l} - \hat{b}_{\mathrm{CV},l}\right)^2}, \tag{S25}$$

$$J_3 = \sqrt{\frac{1}{5}\sum_{j=1}^{5}\left\{\frac{1}{m_{\mathrm{last},j}}\sum_{m=1}^{m_{\mathrm{last},j}}\left(e_j(t_m) - \hat{e}_j(t_m)\right)^2\right\}}, \tag{S26}$$

$$J_4 = \sqrt{\frac{1}{5}\sum_{j=1}^{5}\left\{\frac{1}{m_{\mathrm{last},j}}\sum_{m=1}^{m_{\mathrm{last},j}}\left(e_{75,j}(t_m) - \hat{e}_{75,j}(t_m)\right)^2\right\}}. \tag{S27}$$

$$J_5 = \sqrt{\frac{1}{5}\sum_{j=1}^{5}\left\{\frac{1}{m_{\mathrm{last},j}}\sum_{m=1}^{m_{\mathrm{last},j}}\left(a_j(t_m) - \hat{a}_j(t_m)\right)^2\right\}}, \tag{S28}$$

$$J_6 = \sqrt{\frac{1}{5}\sum_{j=1}^{5}\left\{\frac{1}{m_{\mathrm{last},j}}\sum_{m=1}^{m_{\mathrm{last},j}}\left(a_{\mathrm{CV},j}(t_m) - \hat{a}_{\mathrm{CV},j}(t_m)\right)^2\right\}}. \quad \text{(S29)}$$

The terms, J_1 and J_2, are root mean squared errors (RMSE) of mean values and %CV of baseline levels of biological factors, respectively, J_3 and J_4 are RMSE of the EASI score and EASI-75, respectively, J_5 and J_6 are RMSE of mean values and %CV of *S. aureus* levels, respectively. w_1 to w_6 are the weighting coefficients. $b_{\mathrm{mean},l}$ and $b_{\mathrm{CV},l}$ are the reference values for the mean value and the %CV of baseline levels of the l-th biological factor (l=1,2,3,4). $\hat{b}_{\mathrm{mean},l}$ and $\hat{b}_{\mathrm{CV},l}$ are the corresponding simulated values at the steady state (after 1000 weeks, among 1000 virtual patients). $e_j(t_m)$, $e_{75,j}(t_m)$, $a_j(t_m)$ and $a_{\mathrm{CV},j}(t_m)$ are the reference values of the EASI score, EASI-75, mean *S. aureus* levels and %CV of *S. aureus* levels using the j-th intervention (j=1,2,3,4,5) at time t_m (m=1,…, $m_{\mathrm{last},j}$). $\hat{e}_j(t_m)$, $\hat{e}_{75,j}(t_m)$, $\hat{a}_j(t_m)$ and $\hat{a}_{\mathrm{CV},j}(t_m)$ are the corresponding simulated values. We used $[w_1, w_2, w_3, w_4, w_5, w_6] = [50, 10, 50, 50, 1000, 1]$ with larger weights on some terms (e.g., J_5) that tended to have smaller fitting errors.

The parameters were optimised using differential evolution (Storn and Price, 1997), which is an effective method for global optimisation of a large number of parameters. The conditions for differential evolution were set as follows based on manual trial-and-error.

Mutation constant (F)	: 0.5
Crossover constant (CR)	: 0.7
Strategy	: DE/best/1/bin
Number of population vectors (NP)	: 52
Number of function evaluations (nfe)	: 15652
Number of evaluated generations	: 300
Ranges of parameters searched	: TABLE S2

The *J* reached a plateau value, 569, after the iterative evaluations (FIGURE S). The model fitness was confirmed visually by comparing the reference and simulated data (FIGURE 3).

5. Sensitivity analysis

We conducted a global sensitivity analysis of the model parameters with respect to %improved EASI. We produced 1000 virtual patients by varying the 26 parameters that represent their pathophysiological backgrounds using Latin hypercube sampling (LHS) and computed partial rank correlation coefficient (PRCC) (Marino et al., 2008) between each

parameter and %improved EASI of each treatment. LHS is a sampling method to explore the entire space of multidimensional parameters efficiently, and PRCC represents a rank correlation coefficient that is controlled for confounding effects that could lead to detecting pseudo-correlations. The evaluated ranges of $\ln k_i$ were $[\mu_i - \sigma_i, \mu_i + \sigma_i]$. The *p*-values for the PRCC were adjusted for multiple testing with the Bonferroni procedure, where a significance level of adjusted $p < 0.05$ with an absolute value >0.1 was used.

5.1. Influence of model parameters on efficacy of placebo

Eight model parameters had a significant PRCC with the %improved EASI by placebo (FIGURE S).

Two out of the eight parameters were skin barrier-related (k_3 and b_2). A higher k_3 results in stronger recovery of skin barrier via placebo effects, thereby achieving a higher %improve EASI. A higher b_2 inhibits recovery of skin barrier more strongly, weakening the recovery of the skin barrier by placebo effects, thereby showing lower %improve EASI.

The remaining six parameters were agr-related (k_1, k_4, k_5, b_1, d_5 and d_8). Higher b_1, k_5 and d_5 and lower k_1, k_4 and d_8 result in a lower baseline level of agr expression via decreasing agr expression levels (k_1 and b_1) and *S. aureus* levels (k_4 and d_5) or increasing CoNS levels (k_5 and d_8). A lower level of agr expression means that the % improved EASI score is more sensitive to the changes in the skin barrier integrity that is achieved by placebo effects because we modelled an EASI score as a weighted mean of agr expression and skin barrier integrity (Eq. S13).

These influences were observed in not only placebo groups but also drug-treated groups as the placebo effects were considered in both placebo- and drug-treated groups in the simulation.

5.2. Influence of model parameters on efficacy of dupilumab

Six model parameters had a significant PRCC with the %improved EASI by dupilumab (FIGURE S).

All the six parameters were agr-related (k_1, k_4, k_5, d_4, d_5 and d_8). Higher k_5, d_4 and d_5 and the lower k_1, k_4 and d_8 result in a lower baseline level of agr expression due to a decrease in agr expression (k_1) and in *S. aureus* levels (k_4, d_4 and d_5) or an increase in CoNS levels (k_5 and d_8). A lower level of agr expression means that the % improved EASI score is more sensitive to the changes in the skin barrier integrity that is achieved by placebo effects and dupilumab (inhibiting skin barrier damage from IL-4/IL-13) because we modelled an EASI score as a weighted mean of agr expression and skin barrier integrity (Eq. S13).

Two skin barrier-related parameters (k_3 and b_2) had a significant PRCC with the %improved EASI by placebo, but not by dupilumab, which includes placebo effects in our simulation. It may be because the recovery of the skin barrier by dupilumab overweighted that by placebo effects, and thereby the placebo effects became negligible in dupilumab treatment.

5.3. Influence of model parameters on efficacy of *Sh*A9-sensitive

Seven model parameters had a significant PRCC with the %improved EASI by *Sh*A9-sensitive (FIGURE S).

Two out of the seven parameters were skin barrier-related (k_3 and b_2) and correspond to placebo effects because they had a significant PRCC with the %improved EASI by placebo (SI section 1.1). Other two parameters were bactericidal strengths of *Sh*A9 (d_{A9a_s} and d_{A9h}). A higher d_{A9a_s} and a lower d_{A9h} result in stronger killing of *S. aureus* and weaker killing of CoNS, thereby achieving a higher %improve EASI.

The remaining three parameters were agr-related (k_4, k_5, d_8). As described in SI section 1.1, a lower k_4 showed a higher %improve EASI in placebo treatment. A higher d_8 and a lower k_5 result in a lower baseline level of CoNS. The lower level of CoNS lessens the impact of killing CoNS by *Sh*A9 on the increase of agr expression. The smaller increase in agr expression results in the weaker detrimental effects of *Sh*A9 on EASI scores, thereby showing a higher %improve EASI.

The influences of d_8 and k_5 (i.e., a baseline level of CoNS) on %improve EASI were in opposite directions, depending on whether the drugs kill CoNS (e.g., *Sh*A9 and flucloxacillin) or not (e.g., placebo and dupilumab). A higher baseline level of CoNS makes a lower baseline level of agr expression. The lower level of agr expression means that the %improved EASI score is more sensitive to the changes in the skin barrier integrity that is achieved by placebo and dupilumab because we modelled an EASI score as a weighted mean of agr expression and skin barrier integrity (Eq. S13). On the other hand, a lower level of CoNS lessens the impact of killing CoNS by *Sh*A9 on the increase of agr expression. The smaller increase in agr expression results in the weaker detrimental effects of *Sh*A9 and flucloxacillin on EASI scores, thereby showing a higher %improve EASI.

b_{A9s} (inhibitory strength for agr expression of *S. aureus* via *Sh*A9) had no significant influence on %improve EASI (FIGURE S) because the inhibitory strength of *Sh*A9 for agr expression of *S. aureus* is so weak in this model (i.e., a small μ_i of b_{A9s}) that the sensitivity analysis evaluated a narrow range of inhibition levels of agr expression (The evaluated range of b_{A9s} was 0.25-0.43, 20%-30% around the nominal value). On the other hand, the inhibitory level of agr expression via hypothetical *S. aureus*-targeted therapy had a significant influence on EASI-75 (FIGURE 5) because it evaluated a whole range of inhibition levels of agr expression (0%-100%).

5.4. Influence of model parameters on efficacy of *Sh*A9-resistant

Six model parameters had a significant PRCC with the %improved EASI by *Sh*A9-resistant (FIGURE S).

Two out of the six parameters were skin barrier-related (k_3 and b_2) and correspond to placebo effects because they had a significant PRCC with the %improved EASI by placebo (SI section 1.1). A parameter, d_{A9h}, is the bactericidal strength of *Sh*A9 on CoNS. A lower d_{A9h} results in weaker killing of CoNS, thereby achieving a higher %improve EASI.

The remaining three parameters were agr-related (k_4, d_5 and d_8). As described in SI section 1.1, a higher d_5 and a lower k_4 result in stronger skin barrier recovery by placebo effects, and thereby showed a higher %improve EASI. A higher d_8 result in a lower baseline level of CoNS. The lower level of CoNS lessens the impact of CoNS killing by *Sh*A9 on the increase of agr expression. The smaller increase in agr expression results in weaker detrimental effects of *Sh*A9 on EASI scores, thereby showing a higher %improve EASI.

*Sh*A9-resistant and *Sh*A9-sensitive showed similar results except for k_5, d_5, d_{A9a_s}/d_{A9a_r}; the discrepancy stems from the difference in bactericidal strengths on *S. aureus*.

5.5. Influence of model parameters on efficacy of flucloxacillin

Eight model parameters had a significant PRCC with the %improved EASI by flucloxacillin (FIGURE S).

Two out of the eight parameters were skin barrier-related (k_3 and b_2) and correspond to placebo effects (SI Section 1.1). Other two parameters were bactericidal strengths of flucloxacillin (d_{fa} and d_{fh}). A higher d_{fa} and a lower d_{fh} result in stronger killing of *S. aureus* and weaker killing of CoNS, thereby achieving a higher %improve EASI.

The remaining four parameters were agr-related (k_4, k_5, d_5 and d_8). As described in SI section 1.1, a higher d_5 and a lower k_4 result in stronger recovery of skin barrier via placebo effects, thereby showing a higher %improve EASI. A higher d_8 and a lower k_5 have a lower baseline level of CoNS. The lower level of CoNS lessens the impact of killing CoNS by flucloxacillin on the increase of agr expression. The smaller increase in agr expression results in weaker detrimental effects of *Sh*A9 on EASI scores, thereby showing a higher %improve EASI.

SUPPLEMENTARY TABLES and FIGURES

TABLE S1 Treatments excluded in this study (except for antibiotics/antiseptics)

Treatments	MoA	Clinical efficacies (compared to placebo)	Reasons for exclusion
Bleach bath (hypochlorite 0.005%) (Wong et al., 2013)	Unclear (inhibiting NF-κB?)	Decreased *S. aureus* levels and improved EASI score	Unclear MoA; hypochlorite 0.005% inhibited NF-κB signaling in human keratinocytes, but was not antimicrobial against *S. aureus* (Leung et al., 2013; Sawada et al., 2019).
Vitreoscilla filiformis Lysate (Gueniche et al., 2008)	Unclear (anti-inflammatory?)	Decreased *S. aureus* levels and improved SCORAD	Unclear MoA: target molecules are unknown
Staphefekt (Bacteriophage lysin) (de Wit et al., 2019)	Killing *S. aureus*	Failed to decrease *S. aureus* levels and EASI score compared with placebo	Failed to decrease *S. aureus* levels compared with placebo control
Roseomonas mucosa[Error! Reference source not found.] (Myles et al., 2018)	Producing sphingolipid	Not a placebo-controlled study	Not a placebo-controlled study
Autologous CoNS (Nakatsuji et al., 2021b)	Killing *S. aureus* via bacteriocins	Decreased *S. aureus* levels and improved EASI score	The number of subjects (5-6 subjects/arm) was too small
SRD441 (protease inhibitor) (Foelster et al., 2010)	Inhibiting Staphylococcal-derived aureolysin and matrix metalloproteinases	Slightly improved SCORAD without statistical significance. *S. aureus* levels were not reported	Not reported *S. aureus* levels

TABLE S1 Biological factors as model variables

Model variables		Reported baseline levels in AD lesion, Mean (%CV)		Range
$c_4(t)$	IL-4/IL-13 level at *t*	39.2 (55) (Koppes et al., 2016)[a,c]	Fold change against healthy skin	-
$a(t)$	*S. aureus* level at *t*	3.4 (43) (Nakatsuji et al., 2021a)[b]	Log_{10} CFU/cm^2	0 ~ a_{max}
$h(t)$	CoNS level at *t*	2.0 (84) (Nakatsuji et al., 2021a)[b]	Log_{10} CFU/cm^2	0 ~ h_{max}
$a_{agr}(t)$	Agr expression level at *t*	-[e]	-	0 (no effect) ~ 1 (maximal effect)
$s(t)$	Skin barrier integrity at *t*	-[e]	-	0 (complete destruction) ~ 1 (healthy state)
$e(t)$	EASI score at *t*	29.3 (49)(Blauvelt et al., 2017)[b,c,d]	-	0 ~ 72

a: mild-to-moderate AD patients. Values are average of IL-4 (mean 38.0, %CV 53) and IL-13 (mean 40.5, %CV 56). b: moderate-to-severe AD patients. c: %CV was estimated from IQR. e: no reference data to be compared with simulated values. d: mean baseline value of 29.0 for dupilumab treatment and 29.6 for placebo treatment in dupilumab clinical trial.

TABLE S2 Model parameters

Parameters		Equations	Explored range		Selected values	
			μ_i	σ_i	μ_i	σ_i
k_1	Strength of agr expression	S5	[-2, -1]	[0, 1]	-1.06	0.50
k_2	Recovery rate of skin barrier integrity via skin turnover	S6	[-8, -7]	[0, 1]	-7.71	0.33
k_3	Recovery rate of skin barrier integrity via placebo effects	S6	[-1, 0]	[1, 2]	-0.46	1.58
k_4	Proliferation rate of *S. aureus*	S7	[1, 2]	[0, 1]	1.37	0.20
k_5	Proliferation rate of CoNS	S8	[-2, -1]	[0, 1]	-1.26	0.25
k_6	Secretion rate of IL-4/IL-13 via agr expression	S9	[-9, -8]	[2, 3]	-8.10	2.72
k_7	Secretion rate of IL-4/IL-13 via other pathways	S9	[-6, -5]	[0, 1]	-5.02	0.70
b_1	Inhibitory strength for agr expression via CoNS	S5	[1, 2]	[0, 1]	1.37	0.04

b_2	Inhibitory strength for recovery of skin barrier via IL-4/IL-13	S6	[-3, -2]	[0, 1]	-2.67	0.98
b_3	Inhibitory strength for *S. aureus* proliferation via skin barrier	S7	[-7, -6]	[0, 1]	-6.11	0.60
b_4	Inhibitory strength for elimination of Staphylococci via IL-4/IL-13	S7, S8	[-3, -2]	[1, 2]	-2.71	1.51
d_1	Degradation rate of skin barrier via skin turnover	S6	[-10, -9]	[1, 2]	-9.86	1.41
d_2	Degradation rate of skin barrier via *S. aureus*	S6	[-9, -8]	[2, 3]	-8.33	2.32
d_3	Killing rate of *S. aureus* via bacteriocins secreted from CoNS	S7	[-5, -4]	[2, 3]	-4.65	2.61
d_4	Killing rate of *S. aureus* via AMPs	S7	[0, 1]	[0, 1]	0.55	0.39
d_5	Elimination rate of *S. aureus* via turnover	S7	[0, 1]	[0, 1]	0.23	0.19
d_6	Killing rate of CoNS via bacteriocins secreted from *S. aureus*	S8	[-9, -8]	[0, 1]	-8.14	0.59
d_7	Killing rate of CoNS via AMPs	S8	[-4, -3]	[1, 2]	-3.44	1.88
d_8	Elimination rate of CoNS via turnover	S8	[-2, -1]	[0, 1]	-1.73	0.40
d_9	Elimination rate of IL-4/IL-13	S9	[-9, -8]	[1, 2]	-8.62	1.19
d_{A9a_s}	Killing rate of *S. aureus* via *Sh*A9 in bacteriocin-sensitive *S. aureus*	S13	[1, 2]	[0, 1]	1.09	0.90
d_{A9a_r}	Killing rate of *S. aureus* via *Sh*A9 in bacteriocin-resistant *S. aureus*	S13	[-1, 0]	[0, 1]	-0.83	0.85
d_{A9h}	Killing rate of CoNS via *Sh*A9	S11	[0, 1]	[0, 1]	0.55	0.90
b_{A9s}	Inhibitory strength for agr expression via *Sh*A9	S12	[-2, -1]	[0, 1]	-1.11	0.27
d_{fs}	Killing rate of S. aureus via flucloxacillin	S14	[0, 1]	[0, 1]	0.13	0.27
d_{fh}	Killing rate of CoNS via flucloxacillin	S15	[0, 1]	[0, 1]	0.35	0.12

FIGURE S1 Clinical studies selection process

FIGURE S2 %improved EASI reported in different clinical trials. (left) The relationship between %improved EASI and EASI-75. The placebo data measured at week 16 in a dupilumab Ph2 study (Callewaert et al., 2020) (a black cross) deviates from the data from other clinical trials (all available time points of both drug- and placebo-treated groups in dupilumab Ph3 (Blauvelt et al., 2017), nemolizumab (Kabashima et al., 2020), Tezepelumab (Simpson et al.,2019), GBR 830 (Guttman-Yassky et al., 2019b), lebrikizumab (Guttman-Yassky et al., 2020b) and tralokinumab (Silverberg et al., 2021) studies) and the relationship between the %improved EASI estimated by mixed-effect model repeated measure (MMRM) and EASI-75 measured at week 16 in a dupilumab Ph2 study (Callewaert et al., 2020) (a blue open circle for dupilumab-treated and a black open circle for placebo-treated groups). (right) %improved EASI in dupilumab Ph2 and Ph3 studies. The estimated %improved EASI by MMRM at week 16 in Ph2 (Callewaert et al., 2020) (open circles) is comparable to %improved EASI in Ph3 (Blauvelt et al., 2017) (filled circles) for both dupilumab- and placebo-treated groups.

FIGURE S3 EASI-75 was estimated from %improved EASI using a regression curve. The regression curve was obtained using the reported %improved EASI and EASI-75 in clinical trials of multiple treatments (all available time points of both drug- and placebo-treated groups in dupilumab (Blauvelt et al., 2017), nemolizumab (Kabashima et al., 2020), tezepelumab (Simpson et al., 2019), GBR 830 (Guttman-Yassky et al., 2019b), lebrikizumab (Guttman-Yassky et al., 2020) and tralokinumab (Silverberg et al., 2021)).

FIGURE S4 Agr expression is regulated by *S. aureus* and CoNS

FIGURE S5 Skin barrier integrity is regulated by skin turnover, placebo effects, IL-4/13 and agr expression. Squared and oval symbols represent model variables and implicit factors in our model, respectively.

FIGURE S6 *S. aureus* and CoNS levels regulate each other. Squared and oval symbols represent model variables and implicit factors in our model, respectively.

FIGURE S7 IL-4/IL-13 level is regulated by agr expression and other factors. Squared and oval symbols represent model variables and implicit factors in our model, respectively.

FIGURE S8 EASI score was calculated from agr expression and skin barrier integrity

FIGURE S9 Effects of flucloxacillin. Squared and hexagon symbols represent model variables and a treatment in our model, respectively.

FIGURE S10 Effects of *S. hominis* A9. Squared and hexagon symbols represent model variables and a treatment in our model, respectively.

FIGURE S11 Effects of dupilumab. Squared, oval and hexagon symbols represent model variables, implicit factors and a treatment in our model, respectively.

FIGURE S12 The cost function (J) reached a plateau value, 569, in the optimisation process using differential evolution.

FIGURE S13 Partial rank correlation coefficient (PRCC) between model parameters and %improved EASI by each treatment. Open and crossed cells are statistically significant and non-significant PRCC (absolute value >0.1 with adjusted p-values <0.05), respectively. Positive PRCC means that virtual patients with a higher value of the parameter achieve a higher %improve EASI by the treatment (e.g., k_3). Negative PRCC means that virtual patients with a lower value of the parameter achieve a higher %improve EASI by the treatment (e.g., b_2).